TiS Trends in Sciences
TRENDS IN SCIENCES 2027; 24(1): 13885
SPRINT Scholarly Publishing and Repository Integration Center
https://doi.org/10.48048/tis.2027.13885
RESEARCH ARTICLE

Phytochemical Characterization and Evaluation of Extracts from the Wild Edible Mushroom *Russula emetica* against Herpes Simplex Virus Type 1 (Wild-Type and Drug-Resistant Strains), Human Papillomavirus Type 16 and Cervical Cancer

Wiratchanee Kansandee[1], Padtaya Sirinantananon[2], Chanet Kritsanumphok[2], Keeratikorn Promnikorn[2], Chaleampol Loymunkong[2], Chamsai Pientong[3,4], Tipaya Ekalaksananan[3,4] and Jureeporn Chuerduangphui[2,*]

[1]*Scientific Equipment and Research Division, Kasetsart University Research and Development Institute, Kasetsart University, Bangkok 10900, Thailand*
[2]*Department of Microbiology, Faculty of Science, Kasetsart University, Bangkok 10900, Thailand*
[3]*Department of Microbiology, Faculty of Medicine, Khon Kaen University, Khon Kaen 40002, Thailand*
[4]*HPV & EBV and Carcinogenesis Research Group, Khon Kaen University, Khon Kaen 40002, Thailand*

([*]Corresponding author's e-mail: fscijoc@ku.ac.th)

Received: 21 March 2026, Revised: 20 June 2026, Accepted: 30 June 2026, Published: 15 August 2026

Abstract

Russula emetica is mildly poisonous, but boiling and salt pickling can neutralize its toxins. This mushroom is consumed in some countries, including Thailand. Previous studies on its anticancer compounds are limited, and their potential inhibitory effects against HPV or drug-resistant HSV remain largely unexplored. This study investigated hot water extracts of fresh and dried *R. emetica* fruiting bodies, as well as their freeze-dried counterparts, against HPV-16, HPV-16-positive cervical cancer cells, and HSV-1 (wild-type and drug-resistant strains), and examined potential inhibitory mechanisms. Hot water extraction was performed on fresh and dried fruiting bodies, followed by centrifugation and filtration; half of each water extract was frozen and subjected to freeze-drying. Bioactive compounds in each extract were evaluated using colorimetric assays, HPAEC, and HPLC. FTIR spectroscopy was used to identify functional groups and characterize the chemical composition of the extracts. Cytotoxicity was assessed in Vero, CaSki, and 293FT cell lines. Sub-toxic concentrations were used to evaluate HPV-16 infectivity, E6 expression, CaSki cell growth, and inhibition of HSV-1 KOS drug-susceptible) and HSV-1 dxpIII (drug-resistant). Gene expression profiles in treated cells were examined by RT-PCR. Freeze-dried extracts from fresh fruiting bodies significantly inhibited HSV-1 KOS and HSV-1 dxpIII at the post-entry stage and reduced viral gD mRNA levels and genome copy number. Freeze-dried extracts also significantly reduced HPV-16 E6, *c-fos*, and *YY1* mRNA expression and increased p53 protein levels, suppressed cell migration and colony formation, and promoted cancer cell death. Catechin and rutin identified in *R. emetica* extracts were predicted by molecular docking to exhibit potential binding affinity toward HSV-1 DNA polymerase and HPV-16 E6 proteins. Overall, freeze-dried extracts showed efficacy in inhibiting HSV infection, and suppressing HPV-16 E6 expression and cervical cancer cell growth, suggesting their potential as agents for antiviral activity against HSV and potential anticancer effects in cervical cancer.

Keywords: *Russula emetica*, Human papillomavirus, Herpes simplex virus, Cervical cancer, FTIR, HPAEC, HPLC, Molecular docking

Introduction

Viral infections remain a major global health concern, particularly the high prevalence of certain viruses and drug-resistant strains. Among these, herpes simplex virus and human papillomavirus (HPV) are highly prevalent worldwide and are commonly sexually transmitted infections.

HSV-1 is transmitted through oral contact, oral sex, or sexual intercourse. It primarily causes cold sores on the mouth and face, but some cases present with severe outcomes, including corneal blindness, lymphocytic meningitis, viral encephalitis, and death [1,2]. Globally, more than 3 billion people are HSV-1 positive [3]. The standard treatment is acyclovir (ACV); however, ACV-resistant HSV-1 has been reported in both immunocompetent and immunocompromised patients receiving prolonged therapy, with prevalence estimates of 1.95% - 6.4% [4,5]. In 2019, more than 36.8 million people were living with immunocompromising conditions, particularly human immunodeficiency virus/acquired immune deficiency syndrome. Resistance of HSV-1 to ACV and to other antivirals, including adefovir, cidofovir, foscarnet, and penciclovir, has been reported worldwide [6,7], motivating the search for new anti-HSV agents. These limitations highlight the importance of exploring novel antiviral agents from natural sources, which are rich in diverse bioactive compounds and therapeutic potential.

Human papillomavirus (HPV) is commonly transmitted through oral sex or sexual intercourse. HPV infection can cause several human diseases, and multiple HPV genotypes are associated with sexually transmitted diseases and malignancies [8]. The number of people infected with HPV worldwide is estimated to exceed 290 million [9]. In the United States, 42 million cases of disease-associated HPV infection were recorded, with 13 million new cases diagnosed in 2018 [10]. Cervical cancer is the second most common cause of cancer-related death among women worldwide and in Thailand, with more than 95% of cases associated with HPV infection [11,12]. In addition, current treatments of this cancer are still associated with adverse effects [13]. Although HPV vaccination was first introduced in 2006 and is highly effective in the prevention of cervical cancer and in reducing genital warts and precancerous lesions. It targets only certain HPV types, has not been widely distributed in low- and middle-income countries, and is less effective in preventing HPV-associated cancer development in individuals already infected with this virus [10,14]. Currently, no specific antiviral drug is available to directly eliminate HPV infection. A recent report stated that the herbal product Gene-Eden-VIR/Novirin was reported to be associated with HPV clearance from previous symptomatic viral infection in participants [15]. However, further investigation of natural agents is still needed to elucidate novel bioactive compounds that may inhibit HPV infection and oncogenes, which could contribute to the development of more effective therapeutic approaches.

During the COVID-19 pandemic, health services were overwhelmed by the influx of patients. Therefore, traditional herbal medicine was used to treat COVID-19 patients in many countries, including China and Thailand [16,17]. However, reports of traditional herbal medicine-related adverse effects were common, including headache, dizziness, gastrointestinal discomfort, localized numbness, serious injuries, life-threatening conditions, and death after oral ingestion [18]. Mushrooms have long been used worldwide as herbal medicines to treat a wide range of diseases. In medical applications, research has mainly focused on edible mushrooms because of their relative safety.

Russula emetica (Schaeff.) Pers. (Thai: Hed-Koh-Na-Dang) is a lesser-known medicinal mushroom. This species grows during the rainy season and is consumed in Northeastern Thailand after boiling. Consumption of raw *R. emetica* can induce vomiting [19,20]. Extracts of *R. emetica* have shown moderate antioxidant activity in ethyl acetate fractions and antibacterial effects [21]. Previous studies have also reported health benefits of extracts from the genus *Russula*. For example, *R. alboareolata*, *R. integra*, and *R. lepida* extracts suppressed the growth of cervical cancer (HPV-associated HeLa cells), lung cancer (NCI-H460 cells), hepatoma (HepG2 cells), and breast cancer (MCF-7 cells), respectively, while a peptide from *R. paludosa* reduced HIV-1 reverse transcriptase activity [22,23]. These findings indicate that *Russula*-derived compounds may exert bioactivity across multiple diseases, including both cancers and viral infections. Previous antiviral findings in *Russula* spp. support further exploratory evaluation of *R. emetica* against other clinically relevant viral models, although the underlying mechanisms may differ among HIV, HSV,

and HPV. In addition, the anticancer effects across several kinds of cancer cell lines suggest that *Russula* extracts may influence fundamental cellular processes such as cell proliferation, migration, and apoptosis. Extracts of *Russula*-related species contain various bioactive compounds, including polysaccharides, proteins, flavonoids, and phenolic compounds [24-26], with antioxidant, antimicrobial, antidiabetic, anticancer, and antihypertensive activities [23-25,27]. Notably, several of these compounds have been reported to exhibit antiviral activity against multiple viruses, including HIV-1, HPV, and HSV, as well as anticancer effects, which may suggest their potential broad biological activity and warrant further investigation of *Russula* extracts against a wider range of viral pathogens and cancer-related models [22,28,29].

Despite the increasing use of natural agents for medical applications, there is limited information on anti-HSV, anti-HPV, and anti-cervical cancer cell growth potentials of *R. emetica*. Additionally, no standardized, simple extraction method has been established for obtaining its bioactive compounds. Therefore, this study aimed to evaluate bioactive compounds as well as anti-HSV and HPV infectivity, and anti-cervical cancer cell growth activity of filtered hot water extracts from fresh and dried fruiting bodies of *R. emetica*, which are consumed in Northeastern Thailand. The filtered extracts were further processed either with or without freeze-drying, and these preparation methods were compared to identify a simple and effective approach for obtaining bioactive compounds that may ameliorate HSV- and HPV-associated diseases.

Materials and methods

Mushroom collection, preparation and extraction

R. emetica samples were collected from a tropical forest in Roi Et Province, Thailand, in July 2022 (**Figure S1**) [20]. The fruiting bodies were cut, mashed, and divided into two groups (65 g each). One group was immediately soaked in 65 mL of sterile water and incubated in a boiling water bath for 1 h (Fresh). The other group was dried at 45 °C for 4 d, soaked in 65 mL of sterile water, and incubated in a boiling water bath for 1 h (Dried). The Fresh and Dried solutions were centrifuged at 4,000 rpm for 30 min at 4 °C and filtered using sterile Whatman No. 4 filter paper (Whatman, Maidstone, UK). Half of each solution was frozen and dried (FD) using a SCANVAC CoolSafe^{TM} freeze-dryer (CoolSafe 55, Lynge, Denmark). The dried pellets (FD-Fresh and FD-Dried) were dissolved in 50% DMSO in water to obtain a stock concentration of 250 mg/mL. Extracts prepared without freeze-drying (Wet-Fresh and Wet-Dried) were compared with FD-Fresh and FD-Dried. For non-freeze-dried extracts, concentrations were standardized based on the initial wet weight (Wet) of the mushroom material used for extraction. All extracts were stored at -20 °C until use.

Bioactive compound profiling and antioxidant activity analysis

To comprehensively profile the bioactive compounds in *R. emetica* extracts, this study quantified major constituents, characterized their chemical composition and functional groups, and evaluated their antioxidant activities using the following methods.

Measurement of crude polysaccharide concentration using the phenol-sulfuric acid method

Sixty microliters of each extract were mixed with 60 µL of 6% phenol (Sigma-Aldrich, USA) and incubated for 10 min. Then, 300 µL of 95% - 97% sulfuric acid (EMSURE®, Merck, Darmstadt, Germany) was added, and the mixture was vortexed vigorously. The mixture was dispensed into a 96-well plate (100 µL/well), and absorbance was measured at 490 nm using a spectrophotometer (Multiskan GO, Thermo Scientific™, Vantaa, Finland). Absorbance values were compared with a dextran standard curve (Sigma-Aldrich, MO, USA) generated using different concentrations.

Total protein using the Bradford reagent assay

Protein content was measured by mixing 20 µL of 1:10 diluted extract with 200 µL of 1× Bio-Rad Protein Assay reagent (Bio-Rad Laboratories, Hercules, CA, USA). Absorbance was measured at 595 nm using a spectrophotometer (Multiskan GO). A bovine serum albumin standard curve was generated and used to calculate protein concentrations.

Determination of total tannin content using the vanillin-sulfuric acid method

One hundred microliters of each extract were mixed with vanillin (0.1 mg/mL) in 70% sulfuric acid (v/v) and incubated in the dark at room temperature for 20 min. Absorbance was measured at 540 nm using a spectrophotometer (Multiskan GO). A standard curve was established using different tannin concentrations.

Determination of total terpenoids / phytochemicals using the methanol / chloroform / sulfuric acid method

Five hundred microliters of each extract were mixed with 3.5 mL of ice-cold 95% methanol and centrifuged at 4,000 × *g* for 15 min at room temperature. Two hundred microliters of supernatant were mixed with 1,500 µL chloroform and incubated for 3 min. Then, 100 µL of concentrated sulfuric acid was added, and the mixture was incubated at room temperature for 2 h in the dark. The bottom 200 µL of the reddish-brown phase was collected and mixed with 1,500 µL of 95% methanol. Absorbance was measured at 538 nm using a spectrophotometer (Multiskan GO). Concentrations were calculated using a linalool standard curve (Alfa Aesar, Ward Hill, MA, USA).

High-performance liquid chromatography analysis

To determine the candidate phenolic and flavonoid profiles, a freeze-dried pellet of each extract was dissolved in water (50 mg/mL) and then filtered (0.45 µm) before high-performance liquid chromatography (HPLC) using a Spectra System P-4000 pump (Thermo Separation Products-TSP, Riviera Beach, CA, USA), Spectra System UV-2000 detector, autosampler (Spectra System AS3500), vacuum degasser, and column oven. Ten microliters of each sample were injected into a Phenomenex Luna C18 column (5 µm, 4.6×150 mm), with a guard column used to separate each phenolic compound modified from a previous study [30], using solution A 1% acetic acid and solution B acetonitrile with gradient elution (from 0 - 5 min, linear gradient from 5% to 9% solvent B; 5 - 15 min, held at 9% solvent B; 15 - 22 min, linear gradient from 9% to 11% solvent B; 22 - 38 min, linear gradient from 11% to 18% solvent B; 38 - 43 min, from 18% to 23% solvent B; 43 - 44 min, from 23% to 90% solvent B) and flow rate 1 mL/min. A washing period of 6 min with 80% solvent B and a re-equilibration period of 15 min with 5% solvent B were used between runs. The candidate flavonoid analysis was modified from a previous study [31]. The samples were run with a mobile phase containing solvent A (formic acid solution, pH 2.5) and solvent B (methanol) under gradient elution. The gradient program was as follows: 0 to 20 min, linear gradient from 80% to 30% solvent A; from 20.1 to 22 min, isocratic at 90% solvent B, followed by an 8 min re-equilibration period at 80% solvent A. The analysis was performed using the HPLC apparatus mentioned above.

Fourier transform infrared spectroscopy (FTIR)

The functional groups of *R. emetica* extracts were detected using an INVENIO FTIR Spectrometer (BRUKER, USA). Briefly, the extract powder was blended with anhydrous KBr at a ratio of 1:10 and pressed into a pellet before measurement. Fourier transform infrared spectra were recorded in the range 4,000 - 400 cm^{-1}, with 16 accumulated scans and a resolution of 4 cm^{-1}.

Monosaccharide compositions

Monosaccharide composition was analyzed by high-performance anion exchange chromatography (HPAEC) with pulsed amperometric detection (PAD) after acid hydrolysis. HPAEC was performed on a Dionex ICS-5000 system (Thermo Scientific, USA) coupled with PAD and equipped with a CarboPac PA1 column (4×250 mm). Samples were hydrolyzed with 2 M TFA at 121 °C for 3 h on a heating block. Twenty-five microliters of hydrolyzed sample were injected into the CarboPac PA1 column (4×250 mm). The gradient elution program was as follows: 15.4 mM NaOH at the start; ultrapure water for 4.1 min; 250 mM NaOH for 35.1 min; and 15.4 mM NaOH at 40 min. The column temperature was maintained at 30 °C with a flow rate of 1.0 mL/min. Chromeleon 7.0 software was used for data processing.

2,2-Diphenyl-1-(2,4,6-Trinitrophenyl) hydrazyl (DPPH) radical scavenging assay

DPPH radical scavenging activity was determined by modifying a previously reported method [32]. One milliliter of extract (50 mg/mL) was mixed with 1 mL

of 0.1 mM DPPH solution (Sigma-Aldrich, St. Louis, MO, USA). The mixture was incubated in the dark at room temperature for 30 min, and absorbance at 517 nm was measured using a spectrophotometer (Genesys 180, Thermo Fisher Scientific, Waltham, MA, USA). DPPH radical scavenging activity was expressed as mg GAE/g.

Ferric reducing antioxidant power (FRAP) assay

The FRAP assay was performed as previously described [33]. Briefly, 100 µL of *R. emetica* extract (50 mg/mL) was mixed with 3 mL of FRAP reagent. The reaction mixture was incubated at 37 °C for 4 min, and absorbance was measured at 593 nm using a spectrophotometer. FRAP reagent (Sigma-Aldrich, St. Louis, MO, USA) was prepared from 300 mM sodium acetate buffer (pH 3.6) (Merck, Darmstadt, Germany), 10 mM TPTZ solution (Merck, Darmstadt, Germany), and 20 mM ferric chloride solution (Merck-Schuchardt, Hohenbrunn, Germany) at a ratio of 10:1:1 (v/v/v). The reagent was freshly prepared and warmed to 37 °C before use. Results were expressed as mg GAE/g.

Biological assays

To evaluate the biological activities including antiviral and anti-cervical activities of *R. emetica* extracts, this study investigated their inhibitory effects against HSV and HPV at different stages of viral infection, as well as their anti-growth of cervical cancer, and further investigated the potential mechanisms involved.

Cell culture

HPV-16-positive cervical cancer cell lines CaSki and SiHa were kindly provided by Prof. Tohru Kiyono (National Cancer Center Research Institute, Japan). Human embryonic kidney 293FT and African green monkey kidney Vero cells were purchased from Invitrogen (Carlsbad, CA, USA). All cell lines were cultured in complete medium consisting of DMEM (Gibco, NY, USA) supplemented with 10% FBS (Hyclone Laboratories Inc., Logan, UT, USA) and antibiotics (2.5 µg/mL amphotericin B, 40 µg/mL gentamicin, 100 U/mL penicillin G, and 100 µg/mL streptomycin) and incubated at 37 °C in a humidified atmosphere containing 5% CO_2.

Viruses

HSV-1 strain KOS was kindly provided by Prof. Dr. Pilaipan Puthavathana (Center for Research and Innovation, Faculty of Medical Technology, Mahidol University, Thailand). HSV-1 dxpIII (a phosphonoacetic acid- and phosphonoformate-resistant strain) was kindly obtained from Prof. Donald Coen (Biological Chemistry & Molecular Pharmacology, Harvard Medical School, Boston, MA, USA).

Cytotoxicity by MTT assay

Each cell line (10^4 cells/well) was seeded into a 96-well plate and maintained in a complete medium for 24 h. The extracts were added to the cells at different concentrations (0.10, 0.50, 0.75, 1.00, 2.50, 5.00 and 10.00 mg/mL for FD-Fresh/FD-Dried, and 10.00, 25.00, 50.00, 100.00, 125.00 and 250.00 mg/mL for Wet-Fresh/Wet-Dried) and then incubated for 48 h. Cell absorption viability was assessed using the MTT assay (Invitrogen, Waltham, USA) at 540 nm using a spectrophotometer (Multiskan GO). Untreated, DMSO-treated, and water-treated cells served as negative controls. The cytotoxic concentration at 50% (CC_{50}) was calculated from the dose-response curve between %cell viability and extract concentrations.

HSV inhibition activity in the pre-entry step

Vero cells were seeded in 24-well plates at 10^5 cells/well and incubated for 24 h. HSV-1 KOS or HSV-1 dxpIII at a multiplicity of infection (MOI) of 0.002 were mixed (1:1) with various sub-toxic concentrations of the extracts. The virus–extract mixtures were incubated at 37 °C for 1 h. Then, pre-incubated virus–extract mixtures were added to cells and incubated for 2 h. After washing to remove unbound virus, cells were maintained in complete medium containing 0.5% carboxymethyl cellulose for 48 h. ACV was used as a positive control. Water and DMSO were used as a negative control. Cells were fixed with 10% formaldehyde solution (UNIVAR, Ajax Finechem, Taren Point, Australia) and stained with 0.5% crystal violet in 20% methanol for 50 min. Plaques were counted under a microscope (Nikon ECLIPSE TS100, Japan).

HSV inhibition activity in the post-entry step

Vero cells were seeded in 24-well plates at 10^5 cells/well and incubated for 24 h. HSV-1 KOS or HSV-1 dxpIII at an MOI 0.001 was added and incubated with cells for 2 h. After washing with PBS, each extract at different sub-toxic concentrations, prepared in complete medium containing 0.5% carboxymethyl cellulose, was added to infected cells and incubated for 48 h. ACV was used as a positive control. Water and DMSO were used as a negative control. Plaques were counted under a microscope (Nikon ECLIPSE TS100) after fixation and staining with formaldehyde and crystal violet, as described above.

Production of HPV-16 pseudovirus

293FT cells were seeded in 96-well plates at 3.72×10^3 cells/well (24 wells in total) and incubated for 96 h. 293FT cells were co-transfected with 80 ng/well p16sheLL (expressing recombinant HPV-16 L1 and L2) and 80 ng/well pfwB (expressing green fluorescent protein) (kindly provided by John T. Schiller, Laboratory of Cellular Oncology, Bethesda, MD, USA) using Lipofectamine 2000 (Invitrogen, Carlsbad, CA, USA) for 6 h. At 48 h post-transfection, co-transfected 293FT cells were pooled, harvested and lysed in PBS containing 9.5 mM $MgCl_2$, 0.5% Brij 58 (Sigma-Aldrich, St. Louis, MO, USA), and 0.2% RNase A (bovine pancreas; Sigma Chemical Company, St. Louis, MO, USA). The mixture was incubated for 24 h at 37 °C, and subsequently placed on ice for 5 min. After centrifugation at 1,500 rpm at 4 °C for 5 min, the supernatant was diluted 10-fold and applied to 293FT cells to determine the pseudovirus titer. Green fluorescent-expressing and total cells were observed under a fluorescent microscope (Olympus BX51, Olympus Co., Ltd., Tokyo, Japan) to estimate an MOI.

HPV-16 pseudovirus inhibition activity in the pre-attachment step

293FT cells were incubated at 10^4 cells per well in a 96-well plate for 24 h. HPV-16 pseudovirus at an MOI 0.05 was mixed with Wet-Fresh, Wet-Dried, FD-Fresh, and FD-Dried at sub-toxic concentrations for 1 h at 37 °C and then subjected to the 293FT cells in a 96-well plate for 4 h. After removing the unbound pseudovirus, the mixture was replaced with fresh complete medium and continuously incubated for 48 h. Dextran was used as a positive control. Water and DMSO were used as a negative control. The total and green-fluorescent cells were counted with a hemacytometer under a microscope (Olympus BX51, Olympus, Tokyo, Japan). The percentage of inhibition was calculated by subtracting the percentage of infected cells in the treated and the control groups.

HPV-16 pseudovirus inhibition activity in the adsorption step

293FT at 10^4 cells per well in a 96-well plate were maintained for 24 h. The HPV-16 pseudovirus at MOI 0.05 was loaded to the 293FT cells for 2 h at 20 °C and then removed. The complete medium containing different concentrations of each extract was then subjected to the cells and continuously incubated for 48 h. Dextran was used as a positive control. Water and DMSO were used as a negative control. The total and green-fluorescent cells were counted using a hemacytometer under a microscope (Olympus BX51). The percentage of inhibition was calculated by subtracting the percentage of infected cells in the treated and the control groups.

Anti-growth of HPV-16-positive CaSki using MTT assays

CaSki cell viability was determined using an MTT assay (Invitrogen). Briefly, 5×10^3 cells/well were seeded in 96-well plates and maintained in DMEM containing 2.5% FBS for 24 h. Cells were treated with each extract at various concentrations and incubated for 48 or 96 h. MTT was then added according to the previously described protocol.

Anti-growth of HPV-16-positive CaSki using colony-formation assays

A colony-formation assay was performed using extract-treated CaSki cells seeded at low density. Briefly, 500 cells/well were seeded in 12-well plates and incubated for 24 h. Cells were treated for 48 h with Wet-Fresh and Wet-Dried (100 mg/mL) or FD-Fresh and FD-Dried (2 mg/mL). The medium was then replaced with fresh medium every 3 d until 10 d of incubation. Colonies were fixed and stained with methanol/acetic acid and crystal violet. The percentage of colony formation was calculated as (number of colonies in the

treated group × 100) / (number of colonies in the control group).

Anti-growth of HPV-16-positive CaSki using cell migration assays

Cell migration was assessed using a wound-healing assay. CaSki cells were seeded in 24-well plates at 10^5 cells/well and incubated for 24 h. A wound in the monolayer was generated using a sterile 200 µL tip. After removal of the medium, cells were treated with each extract and incubated for 72 h, with photographs taken on days 0, 1, 2, and 3. Wound distance was measured using ImageJ v1.51j8 (Wayne Rasband, National Institutes of Health, Bethesda, MD, USA).

Anti-growth of HPV-16-positive CaSki using acridine orange/ethidium bromide (AO/EB) assays

Cells exhibiting apoptotic features were assessed by AO/EB staining. CaSki cells were seeded in 24-well plates at 10^5 cells/well and incubated for 24 h. Cells were treated with each extract for 48 h, harvested, and dual-stained with AO/EB (100 µg/mL). Cycloheximide (CHX) was used as a positive control. Water and DMSO were used as a negative control. Cell morphology was observed under a fluorescence microscope (Olympus BX51). Photographs were used to count cells exhibiting normal, necrotic, and apoptotic features in Adobe Photoshop v21.1.0 (Adobe Inc., San Jose, CA, USA) according to the criteria shown (**Figure S2**).

DNA, RNA and protein isolation in the extract-treated cells

DNA was isolated from extract-treated, HSV-1-infected Vero cells using GeneAll® Exgene™ Cell SV Mini Kit (Cat. 106-101, GeneAll Biotechnology Co., Ltd., Seoul, Korea). The HSV-1 *UL30* gene was amplified using a reaction mixture containing 1× SYBR Green master mix (SsoAdvanced™ Universal SYBR® Green Supermix; Bio-Rad, Hercules, CA, USA), 0.3 µM of each specific primer (**Table S1**), and DNA template (40 ng per reaction). Amplification was performed using an Eco48 real-time qPCR system (PCRmax, Staffordshire, UK). Viral copy numbers of HSV-1 KOS and HSV-1 dxpIII (10^9 copies) were serially diluted to 1 - 10^7 copies per reaction to generate a standard curve relating $\log_{10}$ viral copy numbers to cycle threshold (Ct) values. ACV and DMSO were used as positive and negative controls, respectively.

RNA and protein were isolated using TRIzol™ reagent (Thermo Scientific, Waltham, MA, USA) mixed with chloroform (1:0.2 v/v) according to the manufacturer's instructions. The upper phase was collected and mixed with isopropanol to precipitate RNA. The RNA pellet was washed with 75% ethanol, air-dried at room temperature for 30 min, and dissolved in nuclease-free water. Total RNA (200 ng per reaction) was used as a template for cDNA synthesis using the RevertAid First Strand cDNA Synthesis Kit with an oligo(dT) primer (Thermo Fisher Scientific), according to the manufacturer's instructions. mRNA expression levels of cellular and viral genes were determined using specific primers and conditions (**Table S1**). The TRIzol® lower phase remaining after RNA isolation was used for protein extraction according to the manufacturer's instructions. Briefly, the lower layer was mixed with ethanol and centrifuged at 2,000 × g at 4 °C for 5 min to remove DNA. Then, the protein was precipitated by additional isopropanol and centrifuged at 7,500 × g for 5 min at 4 °C. The protein pellet was washed twice with 0.3 M guanidine hydrochloride in 95% ethanol, followed by two washed with absolute ethanol. The protein pellet was air-dried at room temperature for 30 min, and dissolved in rehydration buffer (8M urea and 2% CHAPS). Protein samples were separated by 12% SDS-PAGE and transferred to a nitrocellulose membrane (Amersham Protran 0.2 NC; Cytiva, Marlborough, MA, USA) using a Mini Trans-Blot Cell (Bio-Rad Laboratories, Richmond, CA, USA). After blocking with 5% skim milk and 0.1% Tween 20 in PBS for 1 h, membranes were incubated overnight at 4 °C with primary antibodies against β-actin (1:1,000; clone C4, sc-47778; Santa Cruz Biotechnology, Inc., Santa Cruz, CA, USA) or p53 (1:1,000; clone DO-1; Santa Cruz Biotechnology). Membranes were washed three times with 0.1% Tween 20 in PBS and incubated with IgGκ binding protein-HRP (m-IgGκ BP-HRP) (sc-516102; Santa Cruz Biotechnology). Signals were detected using the ECL™ Western blotting analysis system (CAT No. RPN2109; GE Healthcare, Buckinghamshire, UK) and analyzed using Alliance Q9 (UVITEC, Cambridge, UK).

Molecular docking

To provide computational insights into the potential interactions between candidate bioactive compounds and viral targets, molecular docking analysis was performed to predict binding affinities with a key molecule associated with HSV replication and HPV-induced carcinogenesis. HSV-1 DNA polymerase (PDB ID: 8V1T; accessed 5 February 2025) and HPV-16 E6 (PDB ID: 4GIZ; accessed 16 March 2025) were retrieved from https://www.rcsb.org/. Proteins were processed to remove nonessential molecules using BIOVIA Discovery Studio Visualizer (v21.1.0.20298). Catechin (PubChem CID: 24871278), rutin (PubChem CID: 5280805), vanillic acid (PubChem CID: 8468), and sinapic acid (PubChem CID: 10743) were retrieved from https://pubchem.ncbi.nlm.nih.gov/ (16 March 2025). Docking of ligands to receptors was performed in PyRx (Python Prescription v0.8), with energy minimization applied to all molecules [34]. Grid box dimensions (Å) were set to X = 28.0687, Y = 22.1048, and Z = 29.4790 for HSV-1 DNA polymerase and X = 21.5071, Y = 13.4332, and Z = 17.6900 for HPV-16 E6, corresponding to the active-site binding pockets [35,36]. The docking pose with the lowest binding energy (kcal/mol) and the lowest RMSD was selected. PyMOL (v2.5.7; Schrödinger, LLC) was used to visualize docking results and convert files to PDB format. BIOVIA Discovery Studio Visualizer was used to illustrate interactions in 2D and 3D.

Statistical analysis

Data are presented as mean ± standard error of the mean (SEM) from at least three experiments. Statistical differences were analyzed using a two-tailed Student's t-test for comparisons between two groups, and one-way ANOVA or two-way ANOVA followed by Tukey's post hoc test for multiple comparisons among three or more groups using GraphPad Prism software (version 8.0.2; GraphPad Software Inc., La Jolla, CA, USA). A value of $p < 0.05$ was considered statistically significant. Statistical significance is indicated as $*p < 0.05$, $**p < 0.01$, and $*** p < 0.001$.

Results and discussion

Concentrations of polysaccharides, proteins, tannins, terpenes and sugar compositions in the extract

FD-Fresh showed higher polysaccharide yield, whereas FD-Dried contained greater amounts of protein and total tannins (**Table 1**). DPPH and FRAP activities in FD-Dried were significantly higher than those in FD-Fresh, indicating stronger antioxidant activity in the dried *R. emetica*. The higher DPPH and FRAP activities may be associated mainly with antioxidant-related constituents, particularly tannins and phenolic compounds. Monosaccharide composition of FD-Fresh and FD-Dried hydrolysates was analyzed using HPAEC-PAD as part of a preliminary characterization. In both extracts, glucose was the predominant sugar, followed by galactose and mannose. FD-Fresh contained a glucose proportion of 53.84%, whereas FD-Dried showed 35.18%. In contrast, the proportion of galactose was 33.54% in FD-Dried and 17.26% in FD-Fresh (**Figure S3** and **Table 1**). These values are based on a single analysis and should be interpreted as indicative rather than definitive quantitative differences.

R. emetica is not widely consumed throughout Thailand but is cooked and eaten in certain local areas, particularly in the northeastern region of the country. The mushroom is collected from forests and sold in local markets [37]. This species is not commercially cultivated, although some studies have successfully propagated it [38]. In this study, hot water extraction was used. Cooking the mushroom reduces the contents of carbohydrates, proteins, fats, ash and certain mineral elements, particularly the levels of toxins [39]. A previous study reported that hot water extracts of *R. emetica* contained higher levels of phenolic compounds and exhibited greater antioxidant activity compared to ethanol and methanol [24]. Consistent with previous findings, our results showed that total tannin content (a type of phenolic compound and antioxidant agent) and antioxidant activity in FD-Dried were higher than those in FD-Fresh (**Table 1**). Phenolic compounds, including ferulic, caffeic, p-coumaric, vanillic, and sinapic acids, as well as tannins, flavonoids and terpenoids, are recognized for their antioxidant properties, while other biomolecules, such as lipids, proteins and carbohydrates, are often found in association with phenolic compounds and may modulate their biological

activities [40,41]. Some of these compounds have been reported to demonstrate anti-HSV activity and inhibitory effects on HPV-associated cancers [29,42]. Therefore, these compounds were quantified alongside antioxidant activity using DPPH and FRAP assays, which are well established for evaluating the antioxidant capacity of extracts. This is relevant because oxidative stress is associated with viral infection and cancer development/progression. Kaewnarin *et al.* [24] demonstrated that the *R. emetica* extract obtained by conventional refluxing extraction and ultrasound-assisted extraction exhibited DPPH radical scavenging activities of approximately 9 and 7 mg Trolox/g, respectively, and FRAP reducing power of approximately 10 and 7 mg Trolox/g, respectively. Reis *et al.* [43] reported that the methanolic extract of *R. emetica* showed DPPH and FRAP activities of 1.13 ± 0.01 and 0.69 ± 0.00 mg/mL, respectively, and contained the monosaccharide fructose (0.28 ± 0.17 g/100 g dry weight), which is consistent with our observation [43]. These values differ from our findings, suggesting that extraction methods and the geographical origin of the mushroom may influence its bioactivity. A previous study suggested that the natural polysaccharides MDP-A1 and MDP-A2 extracted from *Menispermumum dauricum*, composed of glucose, mannose, and galactose, have been reported to exhibit antitumor effects in gynecological cancers through induction of caspase-3 and caspase-8 [44]. Notably, these monosaccharides were also identified in our study, which may suggest a possible association with observed biological activity.

Table 1 Concentrations of polysaccharide, protein, tannins, terpenes, anti-oxidant, and monosaccharide composition.

Component	**Yield**	
	FD-Fresh	**FD-Dried**
Extraction yield (mg)	0.848	0.543
Polysaccharide (mg/mL)	9.64 ± 0.30[a]	4.83 ± 0.17[b]
Protein (mg/mL)	0.42 ± 0.12[a]	1.04 ± 0.05[b]
Total tannins (mg/mL)	1.91 ± 0.13[a]	6.44 ± 0.16[b]
Total terpenes (mg/mL)	< 0.079	< 0.079
Anti-oxidation	**Concentration (mg GAE/g)**	
DPPH	0.57 ± 0.15[a]	1.21 ± 0.15[b]
FRAP	1.86 ± 0.01[a]	3.09 ± 0.01[b]
Sugar composition	**Concentration (%)**	
Arabinose	2.16	0.90
Fructose	12.31	10.85
Galactose	17.26	33.54
Glucose	53.84	35.18

Component	Yield	
	FD-Fresh	FD-Dried
Mannose	14.00	19.53
Rhamnose	0.43	0.01

Note: All data are presented as mean ± SEM (n ≥ 3 technical replicates), except for sugar composition analysis, which was performed once. Different mean values between groups were analyzed using a two-tailed Student's t-test. Different superscript letters (a and b) indicate a significant difference between groups ($p < 0.05$).

Phenolic and flavonoid contents in FD-Fresh and FD-Dried

The phenolic and flavonoid profiles of FD-Fresh comprised catechin, protocatechuic acid, rutin, vanillic acid, sinapic acid, ferulic acid, gallic acid, caffeic acid, coumaric acid, and quercetin, ranked from highest to lowest concentration (**Table 2** and **Figure S4**). In contrast, FD-Dried contained catechin, protocatechuic acid, sinapic acid, gallic acid, vanillic acid, ferulic acid, coumaric acid, rutin, caffeic acid, and quercetin (**Table 2** and **Figure S4**). Catechin was the most abundant compound in both extracts, with a higher concentration in FD-Dried than in FD-Fresh (**Table 2**). The nine other abundant compounds detected in both extracts are listed (**Table 2**).

A previous study reported that dried *R. emetica* hot water extract contained 184.9 µg/100 g gallic acid, 2,532.6 µg/100 g protocatechuic acid, 598.7 µg/100 g catechin, 923.3 µg/100 g vanillic acid, and 845.3 µg/100 g rutin, as determined by HPLC. However, although HPLC was similarly employed, the sample preparation differed from that of the present study. Their extracts were not dried, and only the supernatant was directly analyzed [24]. In the present study, FD-Fresh and FD-Dried yielded 19.89 ± 0.85 and 46.58 ± 5.35 µg/mL catechin, respectively, as the most abundant compound among protocatechuic acid, sinapic acid, gallic acid, vanillic acid, ferulic acid, coumaric acid, rutin, caffeic acid, and quercetin (**Table 2**). Catechins, a major group of flavonoids and polyphenols, are bioactive compounds with reported antiviral and anticancer activities. Previous reports showed that catechin directly disrupted HSV particles and inhibited viral replication [45,46]. Catechin also suppressed the growth of cervical cancer cell lines, and its predicted binding to HPV-16 E6 by molecular docking analysis is consistent with our experimental findings [47]. Collectively, these findings suggest that bioactive compounds and nutrients in *R. emetica* may contribute to antimicrobial and anticancer activities. However, limited information is available on the antiviral infectivity and anticancer properties of *R. emetica*. Therefore, this study investigated the effects of *R. emetica* crude extracts on HSV and HPV infectivity, cervical cancer cell growth, and the expression of selected cancer-related genes.

Table 2 Candidate phenolic compounds and flavonoids.

Compound	Concentration (µg/mL)	
	FD-Fresh	FD-Dried
Gallic acid	0.54 ± 0.12[a]	0.54 ± 0.04[a]
Protocatechuic acid	1.89 ± 0.06[a]	3.26 ± 0.19[b]
Vanillic acid	0.93 ± 0.02[a]	0.53 ± 0.02[b]
Caffeic acid	0.44 ± 0.01[a]	0.28 ± 0.01[b]
Coumaric acid	0.37 ± 0.01[a]	0.40 ± 0.03[a]
Ferulic acid	0.55 ± 0.04[a]	0.52 ± 0.03[a]
Sinapic acid	0.86 ± 0.11[a]	0.66 ± 0.03[a]

Compound	Concentration (µg/mL)	
	FD-Fresh	FD-Dried
Catechin	19.89 ± 0.85[a]	46.58 ± 5.35[b]
Rutin	1.87 ± 0.08[a]	0.33 ± 0.05[b]
Quercetin	0.31 ± 0.01[a]	0.08 ± 0.04[b]

Note: All data are presented as mean ± SEM (n = 3 technical replicates). Different mean values between groups were analyzed using a two-tailed Student's t-test. Different superscript letters (a and b) indicate a significant difference between groups ($p < 0.05$).

Fourier transform infrared spectroscopy profiles in FD-Fresh and FD-Dried

To support the characterization of functional groups in FD-Fresh and FD-Dried, the FTIR spectra of FD-Fresh and FD-Dried were compared. Overall, both extracts exhibited similar spectral profiles, except that peaks at 1,456 and 1,026 cm^{-1} were observed only in FD-Fresh (**Figure 1**). A broad band at 3,412 cm^{-1} was observed in both extracts, corresponding to O-H stretching vibration commonly associated with hydroxyl-containing groups [48]. Signals at 2,935 - 2,928 cm^{-1} were attributed to C–H stretching [49]. Amide I was present in both samples, indicated by the strong band at 1,630 cm^{-1} [50]. Bands in the range of 1,600 and 1,400 cm^{-1}, together with the broad O-H band at 3,412 cm^{-1}, are consistent with the presence of aromatic and/or hydroxyl-containing structures. However, these bands are non-specific and may arise from various organic constituents in crude extracts [48,49,51]. Therefore, the presence of polyphenolic compounds cannot be conclusively confirmed based on FTIR alone. Notably, the wavenumber range 1,200 - 800 cm^{-1} is characteristic of carbohydrates and can be used to differentiate polysaccharides [52,53]. As mentioned above, the peaks at 1,456 and 1,026 cm^{-1} detected only in FD-Fresh may be tentatively associated with C-H bending and C-O stretching vibrations, respectively, suggesting the possible presence of carbohydrate- or polysaccharide-related structures [54].

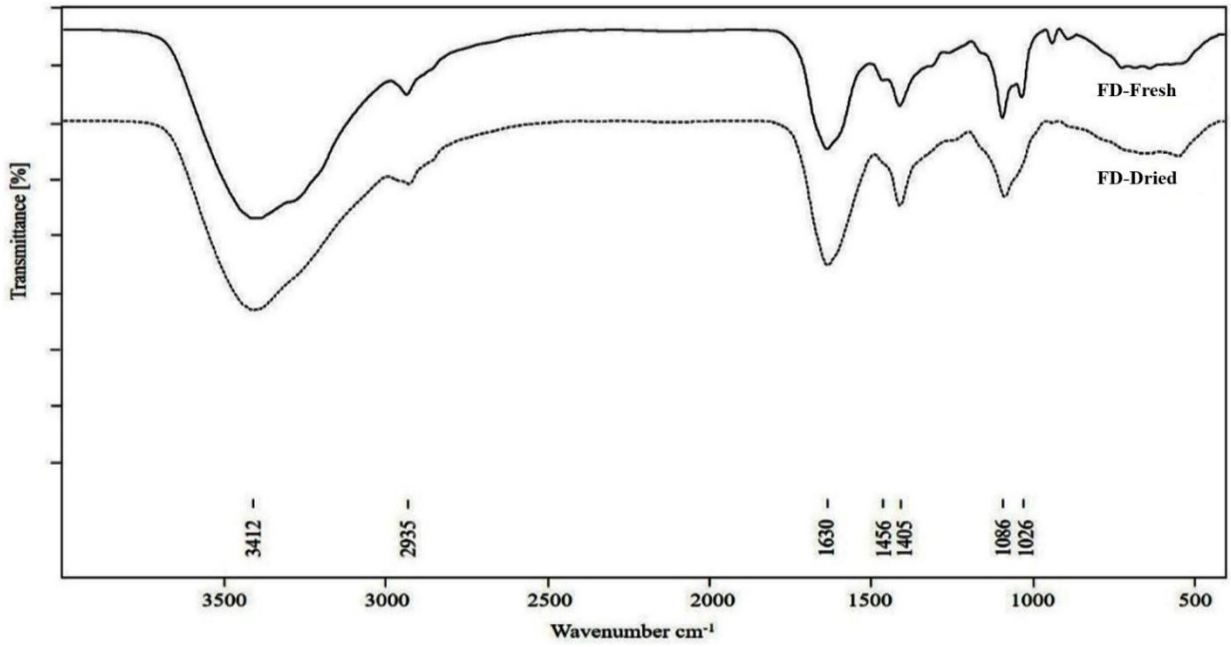


Figure 1 FTIR spectra of *R. emetica* FD-Fresh and FD-Dried extracts. FTIR spectra of FD-Fresh (upper line) and FD-Dried (lower line) were recorded in the range 4,000 - 400 cm^{-1}, using 16 scans at a resolution of 4 cm^{-1}.

Cytotoxicity of Wet-Fresh, Wet-Dried, FD-Fresh and FD-Dried on Vero and CaSki cell lines

Fresh extracts showed lower CC_{50} values than dried extracts, indicating higher cytotoxic potency (**Table S2**). The CC_{50} value of FD-Fresh was lowest in the Vero and CaSki cell lines compared with the others (**Table S2**). Interestingly, all the extracts showed higher cytotoxicity in CaSki and SiHa (**Table S2**) than in Vero, a non-cancerous cell line.

Anti-HSV-1 activity

R. emetica extracts on anti-HSV-1 KOS and HSV-1 dxpIII

Plaque formation in HSV-1 KOS- and HSV-1 dxpIII-infected Vero cells was evaluated following treatment with *R. emetica* extracts at the pre-entry and post-entry steps (**Figure 2** and **Figure S5**). HSV-1 KOS inhibition differed between hot water extracts (Wet-Fresh and Wet-Dried) and freeze-dried extracts (FD-Fresh and FD-Dried) (**Figure 2**). Hot water extracts showed high inhibition (> 80%) in the pre-entry step (**Figure 2(A)**), whereas freeze-dried extracts showed high inhibition (> 80%) in the post-entry step (**Figure 2(B)**). For HSV-1 KOS, the inhibitory concentration at 50% (IC_{50}) of Wet-Fresh and Wet-Dried were 9.186 ± 1.929 and 10.729 ± 1.502 mg/mL, respectively. Simultaneously, IC_{50} values of FD-Fresh and FD-Dried were 0.697 ± 0.120 and 0.819 ± 0.066 mg/mL, respectively. Among these extracts, FD-Dried showed the highest therapeutic potential based on the selectivity index (> 24.406). Because FD-Fresh and FD-Dried showed the lowest IC_{50} values against HSV-1 KOS, their effects against HSV-1 dxpIII were evaluated at the post-entry steps. Both extracts significantly reduced plaque numbers in a dose-dependent manner (**Figure 2(C)** and **Figure S5**). In addition, to further elucidate their possible mechanisms of action at different stages of viral infection, the effects on host-cell receptor binding, viral attachment, penetration, and pre-entry steps were investigated. Notably, neither extract exhibited inhibitory effects against HSV-1 dxpIII at these stages, suggesting that FD-Fresh and FD-Dried may be less effective during early stages of infection and may exert more pronounced effects at the post-entry stage (**Figure S6**).

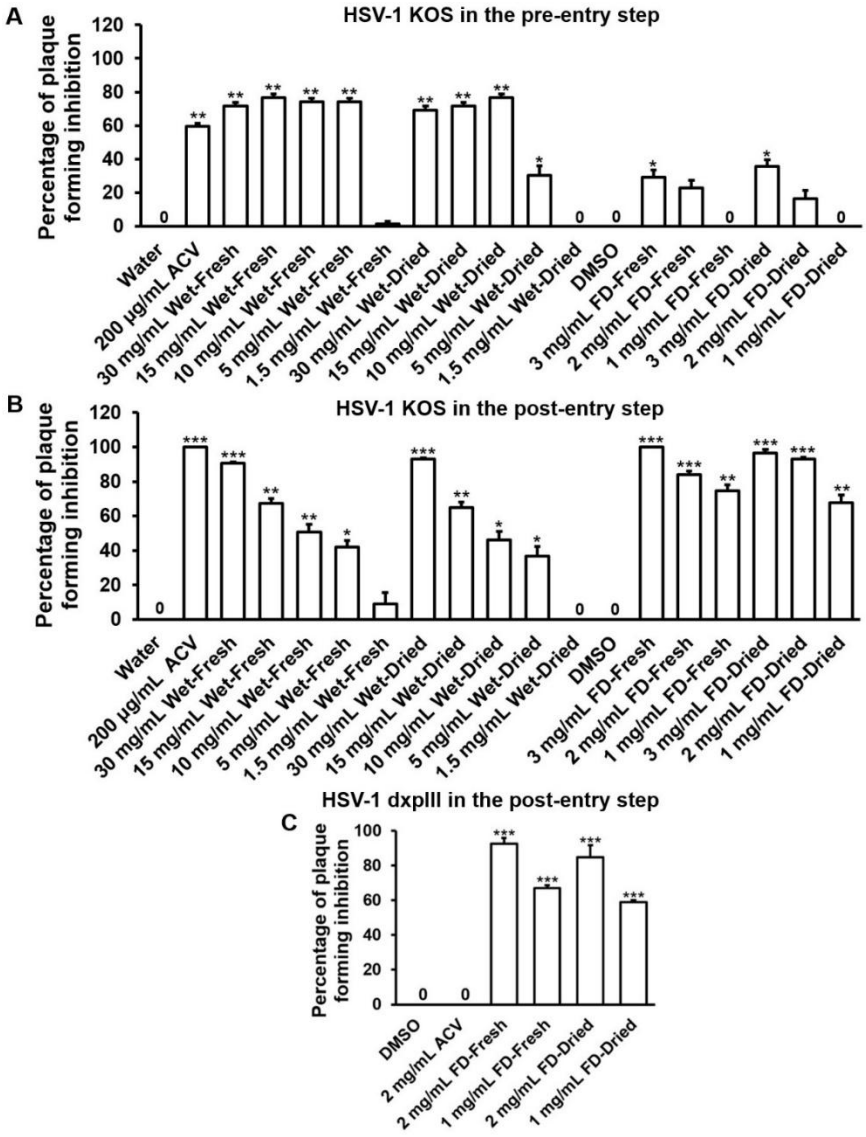


Figure 2 Inhibition of plaque formation in *R. emetica* extract-treated HSV-1 KOS- and HSV-1 dxpIII-infected Vero cells. Anti-HSV-1 KOS activity was evaluated at the pre-entry (A) and post-entry (B) steps. Plaque numbers of HSV-1 dxpIII were measured following treatment with FD-Fresh and FD-Dried (C). All data are presented as mean ± SEM (n = 3 independent biological replicates, each measured in duplicate). Differences in the percentages of plaque-forming inhibition between the study groups were analyzed using one-way ANOVA followed by Tukey's post-hoc multiple comparison test. The symbols * ($p < 0.05$), ** ($p < 0.01$), and *** ($p < 0.001$) indicate significant differences.

R. emetica FD-Fresh and FD-Dried extracts reduced viral gD mRNA levels and copy numbers in HSV-1 KOS and HSV-1 dxpIII-infected Vero cells

To confirm the anti-HSV activity of *R. emetica* extracts against wild-type and drug-resistant strains, viral gD mRNA levels and viral copy numbers were measured by absolute quantification. **Figure 3(A)** shows fold changes in gD mRNA expression in HSV-infected cells treated with FD-Fresh and FD-Dried. Both extracts reduced gD mRNA expression in wild-type and drug-resistant strains relative to the control, with a stronger effect observed for FD-Fresh. Consistent with the gD mRNA results, FD-Fresh (550,267.20 ± 59,201.24 and 34,445.89 ± 509.08 copies/40 ng) significantly reduced viral copy numbers against the wild-type (control: 3,212,946.83 ± 43,2625.71 copies/40 ng, and ACV: 4,212.50 ± 847.63 copies/40 ng) and drug-resistant strains (control: 50,576.98 ± 1,556.11 copies/40 ng, and ACV: 41,234.29 ± 5,443.84 copies/ 40 ng), respectively (**Figure 3(B)**).

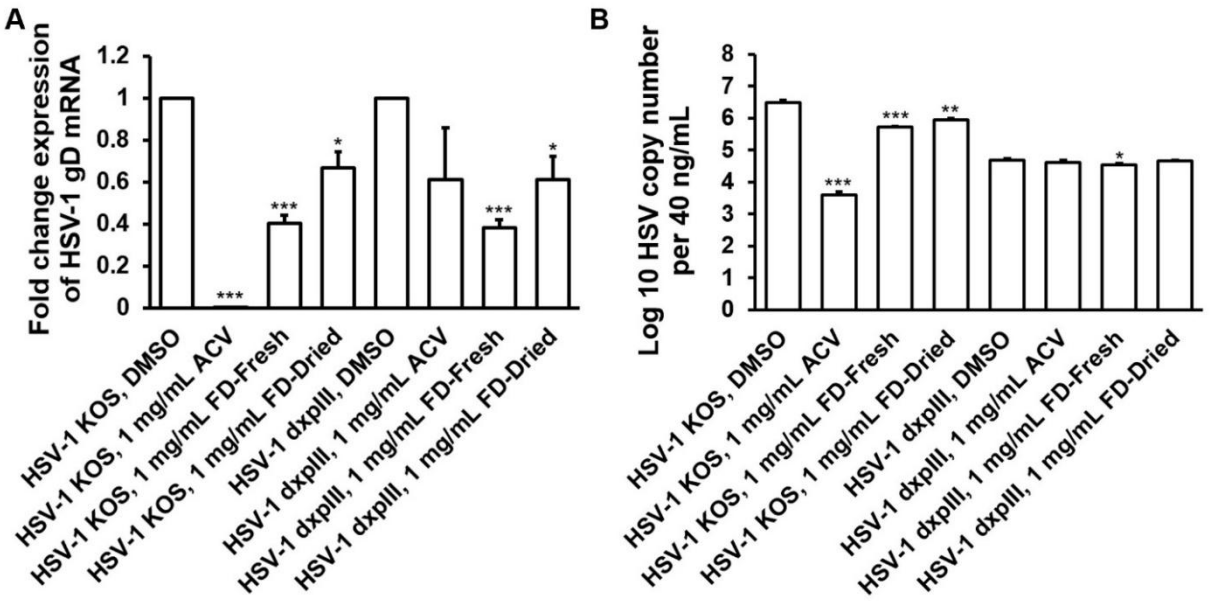


Figure 3 Effects of *R. emetica* extracts on gD mRNA and UL30 DNA copy number in HSV-1 KOS- and HSV-1 dxpIII-infected Vero cells. Infected Vero cells were treated with FD-Fresh or FD-Dried for 48 h, and viral gD mRNA and UL30 DNA copy number were determined by RT-PCR after RNA and DNA extraction. Data are presented as mean ± SEM (n = 3 independent biological replicates, each measured in duplicate). The differences between the study groups were analyzed using one-way ANOVA followed by Tukey's post-hoc multiple comparison test. The symbols * ($p < 0.05$), ** ($p < 0.01$), and *** ($p < 0.001$) indicate significant differences.

HSV infection can be life-threatening, and interest in developing new therapeutic agents has increased. To our knowledge, this study provides the initial evidence for the anti-HSV infection capacity of *R. emetica*. Previous studies reported that *R. emetica* ethanolic extract had anti-HSV-1 and anti-HSV-2 activity, but the antiviral effects were relatively low [55]. By contrast, the present study demonstrated the inhibitory activity against HSV-1, which may be attributed to differences in extraction procedures and assay methods. Our study evaluated crude hot water *R. emetica* extracts containing 4 - 9 mg/mL polysaccharides, which significantly reduced HSV-1 KOS and HSV-1 dxpIII infection. The pre-entry inhibition results suggest that polysaccharides may interact with viral particles [42]. However, both extracts showed less effective plaque reduction at the pre-entry stage (**Figures 2(A) - 2(C)**), suggesting potential intracellular effects, such as interference with viral replication and cellular/viral gene expression. FD-Fresh contained lower levels of proteins, tannins, and antioxidant activities than FD-Dried; however, it tended to show higher inhibitory effects against HSV infection. This suggests that antiviral efficacy may not rely solely on antioxidant activity but could involve additional mechanisms, despite the role of oxidative stress in promoting HSV replication and pathogenesis [56]. The anti-HSV mechanisms of *R. emetica* extracts may involve multiple pathways, including physical interactions and biological regulation. Previous studies reported that *Inonotus obliquus* extract (SI > 80) prevented HSV-1 entry by acting on viral glycoproteins and subsequently inhibiting membrane fusion [57]. In the present study, SI values of *R. emetica* water-based extracts, with or without freeze-drying, were higher than those reported for water-based extracts of *Lentinus edodes* (14.21), *Boletus edulis* (13.96), and *Pleurotus ostreatus* fruiting bodies (15.15) [58]. Sulfated *Agaricus brasiliensis* mycelial polysaccharide has also been reported to inhibit HSV-1 KOS (SI = 439) and HSV-2 (SI = 562) more effectively than non-sulfated *A. brasiliensis* mycelial polysaccharide and dextran sulfate, and its SI against ACV-resistant HSV-1 strains (208) was 69.3-fold higher than that of ACV (> 3) [59].

Anti-HPV and cervical cancer activities

R. emetica extracts reduced CaSki cell proliferation, colony formation, and migration

All Wet-Fresh treatments (10 - 100 mg/mL) significantly reduced the percentage of viable cells at 48 and 96 h, whereas among freeze-dried extracts only FD-Fresh (2 mg/mL) significantly reduced the percentage of viable cells at 48 h. Wet-Dried and FD-Dried showed lower inhibition of cell viability than extracts derived from fresh samples. At 96 h, all extracts significantly reduced the CaSki population in a dose- and time-dependent manner (**Figures 4(A)** - **4(B)**). The highest inhibitory activity was observed with 100 mg/mL Wet-Fresh and 2 mg/mL FD-Fresh, which were subsequently used to evaluate colony formation (single-cell survival) and cell migration. All extracts significantly reduced the number of colonies, with fresh extracts yielding lower colony-formation percentages than dried extracts (**Figures 4(C)** and **S7(A)**). Wet-Fresh, Wet-Dried, and FD-Fresh significantly inhibited cell migration after 48 and 72 h of treatment, whereas FD-Dried did not (**Figures 4(D)** and **S7(B)**). Overall, extracts derived from fresh samples more effectively inhibited CaSki growth than extracts derived from dried samples.

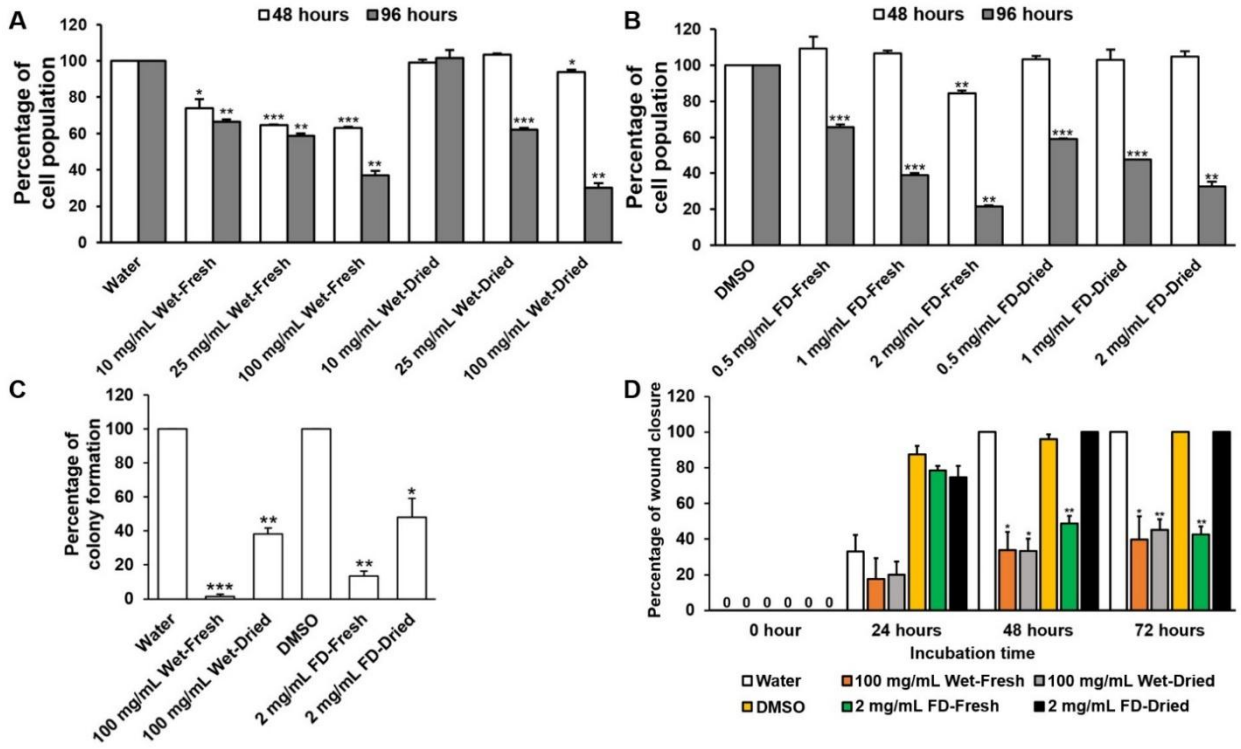


Figure 4 Effects of Wet-Fresh, Wet-Dried, FD-Fresh, and FD-Dried on the growth of CaSki cells. Cell population (A,B), colony formation (C), and cell migration (D) were measured in CaSki cells treated with Wet-Fresh, Wet-Dried, FD-Fresh, or FD-Dried. Data are presented as mean ± SEM (n = 3 independent biological replicates, each measured in duplicate, except for the cell population assay, which was performed in triplicate). The differences between the study group and the control were analyzed using one-way ANOVA or two-way ANOVA followed by Tukey's post hoc test for comparisons among three or more groups. The symbols * ($p < 0.05$), ** ($p < 0.01$), and *** ($p < 0.001$) indicate significant differences.

R. emetica extracts promoted CaSki cell death

All extracts significantly increased the proportion of cells exhibiting apoptotic features to approximately 80%, except for FD-Dried (33.72% ± 1.60%), relative to water (10.82% ± 5.52%) and DMSO (3.36% ± 0.36%). The proportions were 79.94% ± 0.34%, 78.80% ± 1.98%, and 98.82% ± 0.25% for Wet-Fresh, Wet-Dried, and FD-Fresh, respectively (**Figure 5**). Notably, 2 mg/mL FD-Fresh produced the greatest increase in apoptotic cells, particularly late apoptotic cells (90.93% ± 0.19%).

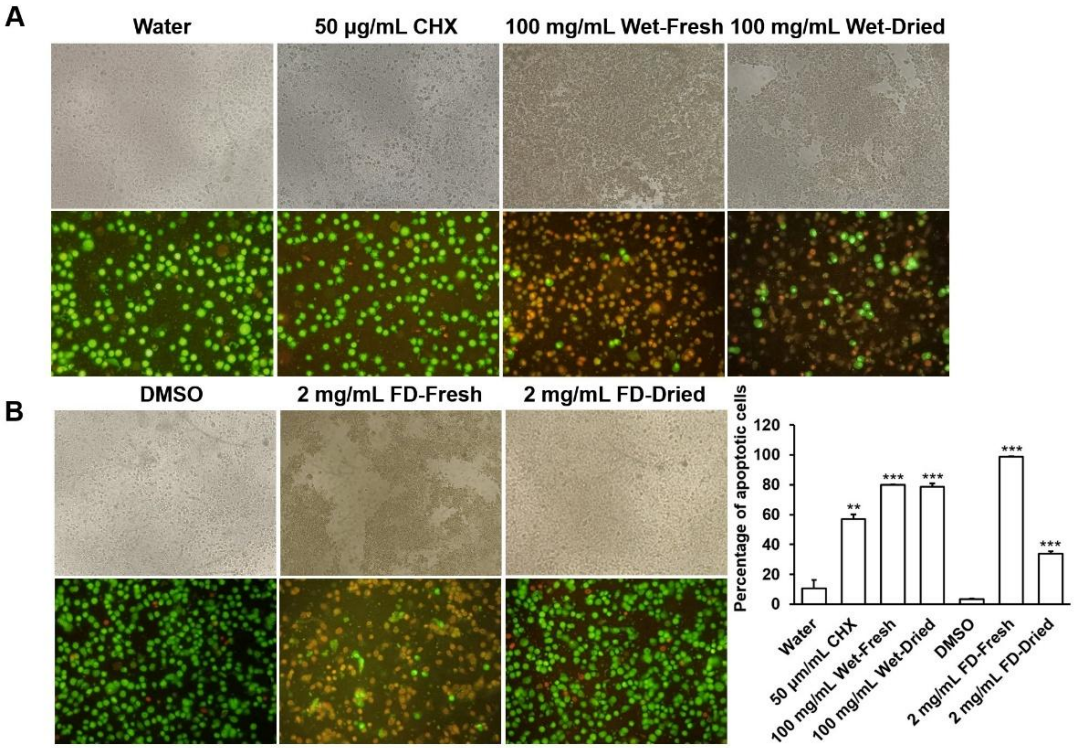


Figure 5 Effects of *R. emetica* extracts on CaSki cell death. CaSki cells were treated with *R. emetica* extracts for 48 h. Cells were stained with AO/EB and observed under a microscope. Cell morphology in CaSki cells treated with Wet-Fresh and Wet-Dried (A) or FD-Fresh and FD-Dried (B) was assessed by light microscopy (10× objective) and fluorescence microscopy (20× objective). The proportion of cells exhibiting apoptotic features was calculated relative to the total cell number. Data are presented as mean ± SEM (n = 3 independent biological replicates, each measured in duplicate). Differences between groups were analyzed using one-way ANOVA followed by Tukey's post hoc multiple-comparison test. The symbols * ($p < 0.05$), ** ($p < 0.01$), and *** ($p < 0.001$) indicate significant differences.

R. emetica extracts suppressed HPV-16 E6 mRNA expression through c-fos and YY1 downregulation

Human transcription factors *c-fos* and *YY1* directly induce expression of the HPV-16 oncogene. HPV-16 has been associated with *c-fos* and *YY1* expression [60,61]. In the present study, Wet-Fresh, Wet-Dried, FD-Fresh, and FD-Dried significantly reduced HPV-16 E6 mRNA levels but did not inhibit viral infection (**Figures 6(A)** and **S8**). Wet-Fresh, FD-Fresh, and FD-Dried significantly reduced *c-fos* mRNA levels, and all extracts reduced *YY1* expression (**Figures 6(B) - 6(C)**). As expected, FD-Fresh at 2 mg/mL significantly increased p53 protein expression, whereas FD-Dried showed a non-significant increasing trend, and these extracts were selected for further investigation because they reduced all three targets, consistent with the reduction in HPV-16 E6 (**Figure S9**).

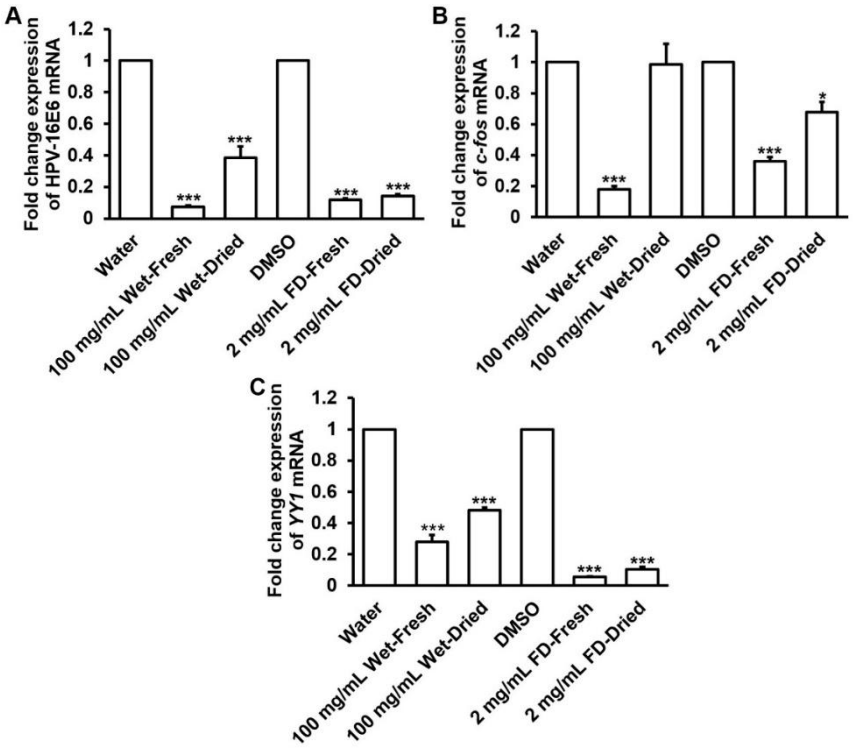


Figure 6 Molecular mechanism underlying the inhibitory effects of Wet-Fresh, Wet-Dried, FD-Fresh, and FD-Dried on HPV-16 E6, *c-fos*, and *YY1* mRNA expression. CaSki cells were treated with Wet-Fresh, Wet-Dried, FD-Fresh, or FD-Dried for 48 h, followed by RNA extraction and cDNA synthesis. HPV-16 E6 (A), *c-fos* (B), and *YY1* mRNA levels (C) were determined by RT-PCR. Data are presented as mean ± SEM (n = 3 independent biological replicates, each measured in duplicate). The differences between the study groups were analyzed using one-way ANOVA followed by Tukey's post-hoc multiple comparison test. The symbols * ($p < 0.05$), and *** ($p < 0.001$) indicate significant differences.

Several phenolic compounds, including flavonoids, phenolic acids, stilbenes, tannins, and lignans, play a role in antioxidant activity and have potential against HPV and cancers [29]. Notably, FD-Fresh potentially showed stronger inhibitory effects on cervical cancer cell growth, while it contained lower levels of most candidate bioactive compounds and antioxidant activities than FD-Dried, consistent with the anti-HSV results (**Figures 4 - 6**). While antioxidants can suppress HPV oncogene expression and the progression of cervical lesions, oxidative stress (OS) has been implicated in HPV-related cervical carcinogenesis [62]. Although the fresh extract exhibits lower antioxidant activity than the dried, the rutin identified in FD-Fresh was 5.67-fold higher than in FD-Dried (**Table 2**). It has been reported to induce OS-mediated apoptosis through p53/Bax/caspase-3 upregulation, along with HPV-18 E6/E7 downregulation of HeLa cells [29]. Therefore, despite lower antioxidant activity, specific bioactive compounds may still exert antiviral and anti-cancer effects. The reduction of CaSki cell viability is consistent with the decreased colony-forming ability, impaired cell migration, and increased cell death population, suggesting that *R. emetica* may contribute to the suppression of cervical cancer cell growth and proliferation. The extracts significantly suppressed HPV-16 E6 mRNA expression in CaSki cells but did not prevent viral infection at the pre-attachment and adsorption steps (**Figures 6(A)** and **S8**). Reduced oncogene expression may be attributable to downregulation of *c-fos* and *YY*1, which are transcription factors that activate the P97 promoter of HPV-16. Some studies have suggested that YY1 acts as a transcriptional repressor of HPV oncogene transcription by quenching AP-1 activity; however, YY1 has also been reported to promote early viral gene expression in HPV-31, and its role in viral oncogene activation and repression remains unclear. These effects may depend on multiple factors, including viral life-cycle status, the stage of cancer development (normal

cervical squamous epithelium progressing to cervical intraepithelial neoplasia), and metastatic progression [63,64]. HPV-18 increased YY1 expression [60]. YY1 is overexpressed in several malignancies, including cervical cancer, and its knockdown in HeLa cells has been reported to increase p53 expression and apoptosis because YY1 binds to p53 and enhances its ubiquitination [64,65]. AP-1 promotes P97 activity to transcribe HPV-16 E6/E7 [61]. The *c-fos* subunit of AP-1 induces HPV-16 oncogene expression and contributes to cervical cancer through multiple mechanisms, including suppression of p53 [61]. TGF-α has been reported to induce *c-fos* expression in an HPV-16 E6-dependent manner [66]. Collectively, these findings suggest that *R. emetica* extracts may reduce *c-fos* and *YY1* expression through upstream and downstream regulation associated with HPV-16 E6/E7, resulting in p53 upregulation and increased apoptosis. Consistent with this interpretation, water-based extracts of *Hexogonia glabra* increased cytotoxicity in CaSki, SiHa, and HeLa cell lines (CC_{50} = 152, 248, and 220 µg/mL, respectively) and increased apoptosis (46 - 79%) through p53 upregulation and downregulation of anti-apoptotic *bcl-2* [67]. Several mushrooms, including *Auricularia auricula-judae*, *Ganoderma applanatum*, and *Sanghuangporus vaninii*, have been reported to decrease anti-apoptotic tendencies and increase pro-apoptotic gene and protein expression [68-70]. A previous study reported that *R. emetica* methanolic extract reduced viability of the multidrug-resistant MES-SA/Dx5 cell line (human uterine sarcoma) through synergy with paclitaxel and interference with P-glycoprotein, an ATP-binding cassette transporter [71].

***In silico* prediction**

The interaction of catechin, rutin, vanillic acid and sinapic acid found in R. emetica extracts and viral targets

The candidate phytochemicals catechin, rutin, vanillic acid, and sinapic acid were predicted to bind directly to HSV-1 DNA polymerase (**Figure 7**). Rutin showed the most favorable binding energy (-9.1 kcal/mol), exceeding that of acyclovir triphosphate, and exhibited the highest predicted affinity for HSV-1 DNA polymerase, followed by catechin (-7.1 kcal/mol), sinapic acid (-5.7 kcal/mol), and vanillic acid (-5.4 kcal/mol) (**Figure 7**).

For HPV-16 E6, rutin showed the most favorable binding energy among the tested phytochemicals (-7.4 kcal/mol) but was less favorable than podophyllotoxin (-8.0 kcal/mol), which is used as an anticancer agent and for treatment of HPV-associated anogenital warts. The LXXLL peptide motif of ubiquitin ligase E6AP interacts with viral E6 [72,73]. Catechin (-7.0 kcal/mol), sinapic acid (-5.4 kcal/mol), and vanillic acid (-4.6 kcal/mol) showed lower predicted affinities than rutin (**Figure 8**). Overall, the docking results provide preliminary computational support for potential interactions between selected compounds and viral targets.

Catechin and rutin, which were among the most abundant phytochemicals detected in *R. emetica* extracts, showed strong predicted binding to HSV-1 DNA polymerase and HPV-16 E6, supporting their potential roles in antiviral activity and in modulation of cellular or viral gene regulation. Protocatechuic acid, the second most abundant compound among the 10 phytochemicals detected by HPLC, could not be analyzed in PyRx because its structure included an “Si” atom, which is not a valid AutoDock atom type.

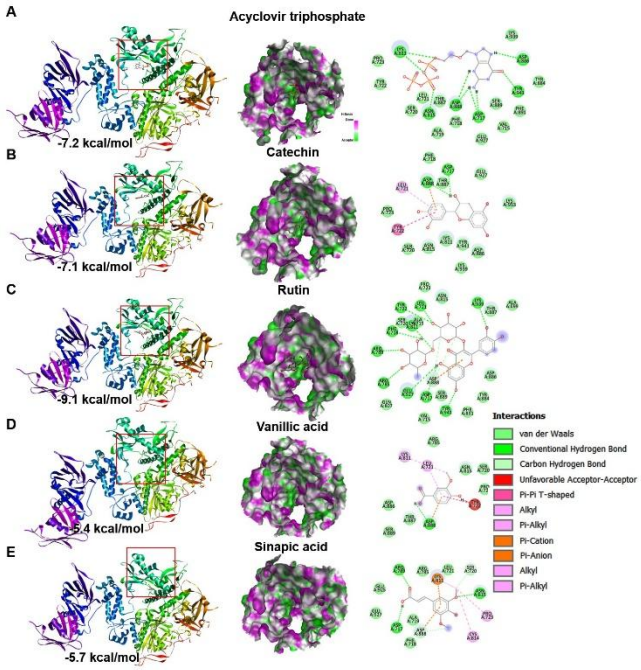


Figure 7 Molecular docking of catechin, rutin, vanillic acid and sinapic acid in *R. emetica* extracts against HSV-1 DNA polymerase. The positive control acyclovir triphosphate was used to reanalyze molecular docking against HSV-1 DNA polymerase in the pocket active binding site (A). Catechin (B), rutin (C), vanillic acid (D), and sinapic acid (E) were analyzed at the same site and grid size as the positive control.

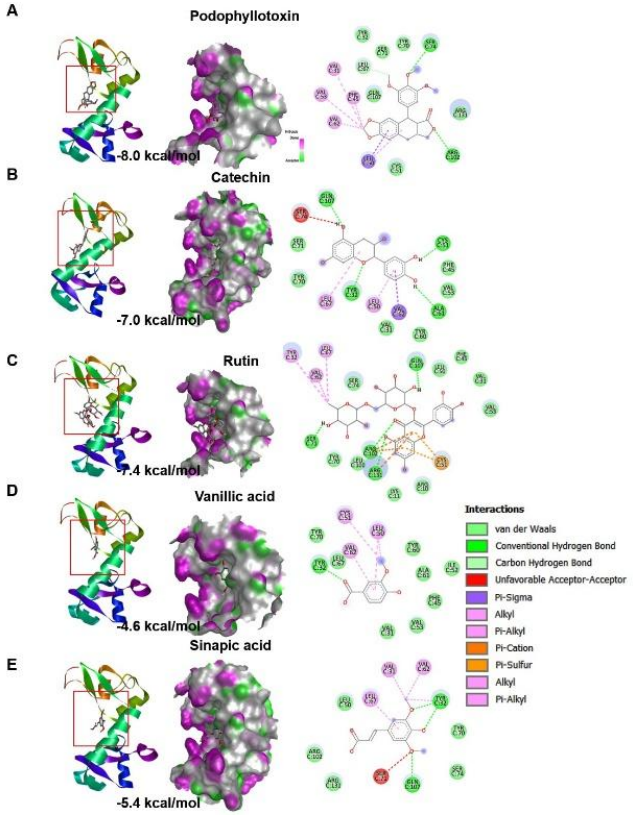


Figure 8 Molecular docking of catechin, rutin, vanillic acid and sinapic acid in *R. emetica* extracts against HPV-16 E6. The positive control podophyllotoxin was used to analyze molecular docking against HPV-16 E6 in the pocket active binding site of the LXXLL peptide binding viral E6 protein (A). Catechin (B), rutin (C), vanillic acid (D), and sinapic acid (E) were analyzed at the same site and grid size as the positive control.

Based on the overall findings, *R. emetica* shows promising antiviral and anti-cervical cancer potential. In this context, it can be hypothesized that increased utilization may raise its demand and promote local cultivation, which might have potential implications for the forest ecosystem [74]. It should be noted that FTIR spectra were intended to provide supportive information on major functional groups rather than definitive compositional analysis. Therefore, advanced spectral analysis, including deconvolution, peak fitting, or semi-quantitative comparison of band intensities, was not performed in this study, which may limit the resolution of overlapping bands in crude extracts. Further studies using these approaches may provide more detailed structural insights. The extracts exhibited antiviral activity against HSV-1, while only limited effects were observed in the HPV-16 pseudoviral model. Notably, the extracts did not inhibit HPV infection at the early stage but significantly reduced HPV-16 E6 expression. Therefore, these findings indicate that the extracts may have viral-specific properties. However, the HPV pseudovirus assay may not fully reflect the overall antiviral effect of the extracts. This system is based on recombinant plasmid-derived pseudovirus and is designed to model early stages of viral entry. In addition, the infectivity of the HPV pseudovirus is dependent on specific cell types, such as 293FT cells. In addition, *in vivo* studies are needed to further investigate and confirm these biological activities as well as to elucidate the pharmacokinetics and safety profiles of *R. emetica* extracts, in order to support their potential future medical application.

Conclusions

This study provides initial evidence that *R. emetica* extracts exhibit antiviral activity against drug-resistant HSV and downregulate HPV-16 E6 expression. Freeze-dried hot water extracts of this mushroom exhibit anti-HSV-1 (including drug-resistant strain), along with anti-cancer effects. In addition, the key compounds identified in this mushroom, such as catechin and rutin, may interact with viral molecules, HSV-1 DNA polymerase and HPV-16 E6 proteins, supporting potential mechanisms of action that require further experimental validation. In addition, the potential synergistic effects of *R. emetica* extracts with the gold standard drug or therapies for HSV or HPV-associated cancer should be evaluated in future study. Overall, these findings highlight the potential of *R. emetica* extracts as natural antiviral and anti-cancer agents.

Acknowledgements

We would like to thank UGSAS-GU via the "Microbiology Laboratory Station for IC-GU12" at Kasetsart University, Thailand.

Declaration of Generative AI in Scientific Writing

ChatGPT (OpenAI) was used solely to improve the readability during manuscript preparation. No scientific content or data interpretation was generated by AI. The authors take full responsibility for the content.

CRediT Author Statement

Wiratchanee Kansandee: Methodology; Software; Validation; Formal analysis; Investigation; Data Curation; Writing - Original Draft; Writing - Review & Editing; Visualization. **Padtaya Sirinantananon**: Methodology; Investigation; Data curation; Writing - Review & Editing. Validation. **Chanet Kritsanumphok**: Investigation; Data curation; Writing - Original draft preparation; Writing - Review & Editing. **Keeratikorn Promnikorn**: Investigation; Data curation; Writing - Original draft preparation; Writing - Review & Editing. **Chaleampol Loymunkong**: Investigation; Original draft preparation; Writing - Review & Editing. **Chamsai Pientong**: Validation; Original draft preparation; Writing - Review & Editing. **Tipaya Ekalaksananan**: Validation; Original draft preparation; Writing - Review & Editing. **Jureeporn Chuerduangphui**: Conceptualization; Methodology; Software; Validation; Formal analysis; Investigation; Resources; Original draft preparation; Writing - Review & Editing; Visualization; Supervision; Project administration; Funding acquisition.

References

[1] A Pandit, SK Shrivastava and S Sethi. Contemporary challenges in sexually transmitted diseases: From diagnostics to drug resistance. *Venereology* 2026; **5(2)**, 14.

[2] C Loymunkong, K Choowongkomon, C Heawchaiyaphum, N Chatchawankanpanich, C Pientong, T Ekalaksananan and J Chuerduangphui. Anti-herpes simplex virus (wild-type and drug-resistant) properties of herbal Kerra™, KS™, and Minoza™. *Viruses* 2025; **17(7)**, 889.

[3] C James, M Harfouche, NJ Welton, KM Turner, LJ Abu-Raddad, SL Gottlieb and KJ Looker. Herpes simplex virus: Global infection prevalence and incidence estimates, 2016. *Bulletin of the World Health Organization* 2020; **98(5)**, 315-329.

[4] R Duan, RD de Vries, AD Osterhaus, L Remeijer and GMGM Verjans. Acyclovir-resistant corneal HSV-1 isolates from patients with herpetic keratitis. *The Journal of Infectious Diseases* 2008; **198(5)**, 659-663.

[5] R Stránská, R Schuurman, E Nienhuis, IW Goedegebuure, M Polman, JF Weel, PM Wertheim-Van Dillen, RJ Berkhout and AMV Loon. Survey of acyclovir-resistant herpes simplex virus in the Netherlands: Prevalence and characterization. *Journal of Clinical Virology* 2005; **32(1)**, 7-18.

[6] J Piret and G Boivin. Resistance of herpes simplex viruses to nucleoside analogues: Mechanisms, prevalence, and management. *Antimicrobial Agents and Chemotherapy* 2011; **55(2)**, 459-472.

[7] TH Bacon, MJ Levin, JJ Leary, RT Sarisky and D Sutton. Herpes simplex virus resistance to acyclovir and penciclovir after two decades of antiviral therapy. *Clinical Microbiology Reviews* 2003; **16(1)**, 114-128.

[8] J Lopes-Nunes, M Lopes, B Rosado, IG Maocha, J Rolo, C Gaspar, B Pires, T Rosado, E Gallardo, A Palmeira-de-Oliveira, J Martinez-de-Oliveira, C Ferreira, MPC Campello, A Paulo, B Medeiros-Fonseca, L Félix, C Venâncio, MDL Pinto, PA Oliveira, R Palmeira-de-Oliveira and C Cruz. Vaginal formulation development: A strategy based on aptamer-guided liposome for human papillomavirus-induced lesions. *European Journal of Pharmaceutics and Biopharmaceutics* 2025; **210**, 114693.

[9] S Sethi, A Ali, X Ju, A Antonsson, R Logan, K Canfell, M Smith, G Garvey, J Hedges and L Jamieson. A systematic review and meta-analysis of the prevalence of human papillomavirus infection in Indigenous populations–A Global Picture. *Journal of Oral Pathology & Medicine* 2021; **50(9)**, 843-854.

[10] RM Lewis, JF Laprise, JW Gargano, ER Unger, TD Querec, HW Chesson, M Brisson and LE Markowitz. Estimated prevalence and incidence of disease-associated human papillomavirus types among 15-to 59-year-olds in the United States. *Sexually Transmitted Diseases* 2021; **48(4)**, 273-277.

[11] X Meng, B Yang, H Yin, J Chen, W Ma, Z Xu and Y Shen. Global burden and incidence trends in cancers associated with human papillomavirus infection: A Population-based systematic study. *Pathogens* 2025; **14(9)**, 880.

[12] M Brisson and M Drolet. Global elimination of cervical cancer as a public health problem. *The Lancet Oncology* 2019; **20(3)**, 319-321.

[13] M Palagudi, S Para, N Golla, KC Meduri, SP Duvvuri, Y Vityala, DC Sajja and U Damineni. Adverse effects of cancer treatment in patients with cervical cancer. *Cureus* 2024; **16(2)**, e54106.

[14] LE Markowitz, V Tsu, SL Deeks, H Cubie, SA Wang, AS Vicari and JM Brotherton. Human papillomavirus vaccine introduction–the first five years. *Vaccine* 2012; **30(S5)**, F139-F148.

[15] H Polansky, E Itzkovitz and A Javaherian. Human papillomavirus (HPV): Systemic treatment with Gene-Eden-VIR/Novirin safely and effectively clears virus. *Drug Design, Development and Therapy* 2017; **11**, 575-583.

[16] N Chaomuang, AJ Dede, S Saokaew and A Umnuaypornlert. Effects of home drug delivery on drug-related problems: Preliminary evidence for improved patient outcomes during the COVID-19 pandemic in Thailand. *Journal of the American Pharmacists Association* 2022; **62(4)**, 1206-1213.

[17] B Yan, Z Jiang, J Yuan, M Li, J Zeng, J Tang, ZK Lu, H Ding, J Xia and Q Wang. Effects and safety of herbal medicines among community-dwelling residents during COVID-19 pandemic: A large prospective, randomized controlled trial (RCT). *Phytomedicine* 2021; **85**, 153403.

[18] M Ekor. The growing use of herbal medicines: Issues relating to adverse reactions and challenges

in monitoring safety. *Frontiers in Pharmacology* 2014; **4**, 177.

[19] P Radford. Fungi, food, poison and mystery. *Bristol Medico-Chirurgical Journal* 1982; **97(3-4)**, 12-15.

[20] T Yuwa-Amornpitak and PN Yeunyaw. Diversity of wild mushrooms in the community forest of Na Si Nuan sub-district, Thailand. *Journal of Biochemical Technology* 2020; **11(3)**, 28-36.

[21] P Klungsupya. Apoptotic activity of ethanolic extract of Thai indigenous mushroom *Russula alboareolata* against L929, HeLa and HepG2 cells by MMP assay. *Thai Journal of Pharmaceutical Sciences* 2016; **40**, 123-126.

[22] J Wang, H Wang and TB Ng. A peptide with HIV-1 reverse transcriptase inhibitory activity from the medicinal mushroom *Russula paludosa*. *Peptides* 2007; **28(3)**, 560-565.

[23] J Yang, SC Karunarathna, N Patabendige, E Tarafder, D Lou, Y Zhou and K Hapuarachchi. Unveiling the bioactive compounds and therapeutic potential of *Russula*: A comprehensive review. *Journal of Fungi* 2025; **11(5)**, 341.

[24] K Kaewnarin, N Suwannarach, J Kumla and S Lumyong. Phenolic profile of various wild edible mushroom extracts from Thailand and their antioxidant properties, anti-tyrosinase and hyperglycaemic inhibitory activities. *Journal of Functional Foods* 2016; **27**, 352-364.

[25] K Kaewnarin, N Suwannarach, J Kumla, S Choonpicharn, K Tanreuan and S Lumyong. Characterization of polysaccharides from wild edible mushrooms from Thailand and their antioxidant, antidiabetic, and antihypertensive activities. *International Journal of Medicinal Mushrooms* 2020; **22(3)**, 221-233.

[26] Y Cheng, J Gan, B Yan, P Wang, H Wu and C Huang. Polysaccharides from *Russula*: A review on extraction, purification, and bioactivities. *Frontiers in Nutrition* 2024; **11**, 1406817.

[27] S Jiamworanunkul and P Chomcheon. Screening of antimicrobial and antioxidant properties of ethyl acetate extracts from wild edible mushrooms. *Thai Journal of Pharmaceutical Sciences* 2015; **43(3)**, 161-167.

[28] DJ Seo and C Choi. Antiviral bioactive compounds of mushrooms and their antiviral mechanisms: A review. *Viruses* 2021; **13(2)**, 350.

[29] A Arab, F Amini, A Iraji and MH Hashempur. The potential of polyphenols and polyphenol-rich extracts against human papillomavirus infections and associated cancers. *Journal of Functional Foods* 2025; **129**, 106873.

[30] S Butsat and S Siriamornpun. Phenolic acids and antioxidant activities in husk of different Thai rice varieties. *Food Science and Technology International* 2010; **16(4)**, 329-336.

[31] X Zhang, Z Wu, P Weng and Y Yang. Analysis of tea catechins in vegetable oils by high-performance liquid chromatography combined with liquid–liquid extraction. *International Journal of Food Science and Technology* 2015; **50(4)**, 885-891.

[32] Y Su and L Li. Structural characterization and antioxidant activity of polysaccharide from four auriculariales. *Carbohydrate Polymers* 2020; **229**, 115407.

[33] S Fiorentino, L Bellani, M Santin, A Castagna, MC Echeverria and L Giorgetti. Effects of microalgae as biostimulants on plant growth, content of antioxidant molecules and total antioxidant capacity in *Chenopodium quinoa* exposed to salt stress. *Plants* 2025; **14(5)**, 781.

[34] O Trott and AJ Olson. AutoDock Vina: Improving the speed and accuracy of docking with a new scoring function, efficient optimization, and multithreading. *Journal of Computational Chemistry* 2010; **31(2)**, 455-461.

[35] K Zanier, S Charbonnier, AOMHO Sidi, AG McEwen, MG Ferrario, P Poussin-Courmontagne, V Cura, N Brimer, KO Babah, T Ansari, I Muller, RH Stote, J Cavarelli, SV Pol and G Travé. Structural basis for hijacking of cellular LxxLL motifs by papillomavirus E6 oncoproteins. *Science* 2013; **339(6120)**, 694-698.

[36] S Shankar, J Pan, P Yang, Y Bian, G Oroszlán, Z Yu, P Mukherjee, DJ Filman, JM Hogle, M Shekhar, DM Coen and J Abraham. Viral DNA polymerase structures reveal mechanisms of antiviral drug resistance. *Cell* 2024; **187(20)**, 5572.e15-5586.e15.

[37] M Manassila, T Sooksa-Nguan, N Boonkerd, S Rodtong and N Teaumroong. Phylogenetic diversity of wild edible *Russula* from northeastern Thailand on the basis of internal transcribed spacer sequence. *Science Asia* 2005; **31**, 323-328.

[38] A Morselt, WTM Smits and T Limonard. Histochemical demonstration of heavy metal tolerance in ectomycorrhizal fungi. *Plant and Soil* 1986; **96(3)**, 417-420.

[39] Y Yusran, E Erniwati, H Maksum, A Khumaidi and R Setiarto. Effect of cooking on the proximate composition and minerals content of wild edible macro fungi from Lore Lindu National Park, Central Sulawesi, Indonesia. *African Journal of Food, Agriculture, Nutrition and Development* 2022; **22(5)**, 20523-20541.

[40] L Jakobek. Interactions of polyphenols with carbohydrates, lipids and proteins. *Food Chemistry* 2015; **175**, 556-567.

[41] N Bibi Sadeer, D Montesano, S Albrizio, G Zengin and MF Mahomoodally. The versatility of antioxidant assays in food science and safety—Chemistry, applications, strengths, and limitations. *Antioxidants* 2020; **9(8)**, 709.

[42] X Zhong, Y Zhang, M Yuan, L Xu, X Luo, R Wu, Z Xi, Y Li and H Xu. *Prunella vulgaris* polysaccharide inhibits herpes simplex virus infection by blocking TLR-mediated NF-κB activation. *Chinese Medicine* 2024; **19(1)**, 6.

[43] FS Reis, E Pereira, L Barros, MJ Sousa, A Martins and ICFR Ferreira. Biomolecule profiles in inedible wild mushrooms with antioxidant value. *Molecules* 2011; **16(6)**, 4328-4338.

[44] Y Li, C Zhang, L Feng, Q Shen, F Liu, X Jiang and B Pang. Application of natural polysaccharides and their novel dosage forms in gynecological cancers: Therapeutic implications from the diversity potential of natural compounds. *Frontiers in Pharmacology* 2023; **14**, 1195104.

[45] CE Isaacs, GY Wen, W Xu, JH Jia, L Rohan, C Corbo, VD Maggio, EC Jenkins and S Hillier. Epigallocatechin gallate inactivates clinical isolates of herpes simplex virus. *Antimicrobial Agents and Chemotherapy* 2008; **52(3)**, 962-970.

[46] AD Oliveira, SD Adams, LH Lee, SR Murray, SD Hsu, JR Hammond, D Dickinson, P Chen and TC Chu. Inhibition of herpes simplex virus type 1 with the modified green tea polyphenol palmitoyl-epigallocatechin gallate. *Food and Chemical Toxicology* 2013; **52**, 207-215.

[47] G Uwanyagasani, E Song'Oro, J Ndacyayisenga, EM Terefe and J Muriuki. *In vitro* activity of various Kenyan tea extracts against HeLa human cervical cancer cell line and molecular docking of tea catechins on high-risk HPV16E6 protein. *Informatics in Medicine Unlocked* 2024; **44**, 101420.

[48] S Khatua, AK Dutta, S Chandra, S Paloi, K Das and K Acharya. Introducing a novel mushroom from mycophagy community with emphasis on biomedical potency. *PLoS One* 2017; **12(5)**, e0178050.

[49] L Dou, X Zhang, MM Zangeneh and Y Zhang. Efficient biogenesis of Cu_2O nanoparticles using extract of *Camellia sinensis* leaf: Evaluation of catalytic, cytotoxicity, antioxidant, and anti-human ovarian cancer properties. *Bioorganic Chemistry* 2021; **106**, 104468.

[50] S Suresh, S Karthikeyan and K Jayamoorthy. FTIR and multivariate analysis to study the effect of bulk and nano copper oxide on peanut plant leaves. *Journal of Science: Advanced Materials and Devices* 2016; **1(3)**, 343-350.

[51] S Wang, Y Wang, Q Cai, X Wang, H Jin and Z Luo. Multi-step separation of monophenols and pyrolytic lignins from the water-insoluble phase of bio-oil. *Separation and Purification Technology* 2014; **122**, 248-255.

[52] H Cao, X Wang, M Shi, X Guan, C Zhang, Y Wang, L Qiao, H Song and Y Zhang. Influence of physicochemical changes and aggregation behavior induced by ultrasound irradiation on the antioxidant effect of highland barley β-glucan. *Food Chemistry: X* 2023; **19**, 100793.

[53] W Kansandee, S Moonmangmee, S Vangpikul, P Kosawatpat and M Tamtin. Physicochemical properties and *in vitro* prebiotic activity of *Ulva rigida* polysaccharides. *Biocatalysis and Agricultural Biotechnology* 2024; **59**, 103252.

[54] N Marcin, V Thesnor, V Duvauchelle, A Ponce-Mora, L Gimeno-Mallench, S Narayanin-Richenapin, L Brelle, E Bejarano, C Yacou, M Sylvestre, C Onésippe-Potiron, P Meffre, Z Benfodda and G Cebrian-Torrejon.

Characterization of alginates of *Sargassum* from the archipelago of Guadeloupe. *Separations* 2024; **11(8)**, 226.

[55] M Amoros, J Boustie, ML Py, V Hervé and V Robin. Antiviral activity of Homobasidiomycetes: Evaluation of 121 Basidiomycetes extracts on four viruses. *International Journal of Pharmacognosy* 1997; **35(4)**, 255-260.

[56] J Sutter, PJ Bruggeman, B Wigdahl, FC Krebs and V Miller. Manipulation of oxidative stress responses by non-thermal plasma to treat herpes simplex virus type 1 infection and disease. *International Journal of Molecular Sciences* 2023; **24(5)**, 4673.

[57] HH Pan, XT Yu, T Li, HL Wu, CW Jiao, MH Cai, XM Li, YZ Xie, Y Wang and T Peng. Aqueous extract from a Chaga medicinal mushroom, *Inonotus obliquus* (higher basidiomyetes), prevents herpes simplex virus entry through inhibition of viral-induced membrane fusion. *International Journal of Medicinal Mushrooms* 2013; **15(1)**, 29-38.

[58] S Santoyo, AC Ramírez-Anguiano, L Aldars-García, G Reglero and C Soler-Rivas. Antiviral activities of *Boletus edulis*, *Pleurotus ostreatus* and *Lentinus edodes* extracts and polysaccharide fractions against herpes simplex virus type 1. *Journal of Food & Nutrition Research* 2012; **51(4)**, 225-235.

[59] FTGDS Cardozo, CM Camelini, A Mascarello, MJ Rossi, RJ Nunes, CRM Barardi, MMD Mendonça and CMO Simões. Antiherpetic activity of a sulfated polysaccharide from *Agaricus brasiliensis* mycelia. *Antiviral Research* 2011; **92(1)**, 108-114.

[60] H Liu, J Xu, Y Yang, X Wang, E Wu, V Majerciak, T Zhang, RDM Steenbergen, HK Wang, NS Banerjee, Y Li, W Lu, C Meyers, J Zhu, X Xie, LT Chow and ZM Zheng. Oncogenic HPV promotes the expression of the long noncoding RNA lnc-FANCI-2 through E7 and YY1. *Proceedings of the National Academy of Sciences* 2021; **118(3)**, e2014195118.

[61] J Chuerduangphui, C Loymunkong, T Ekalaksananan and C Pientong. Arecoline, a main alkaloid in *Areca catechu*, induces biological changes in human papillomavirus 16-positive cervical cancer cells via upregulation of viral oncogenes and cellular transcriptional factors. *Asian Pacific Journal of Tropical Biomedicine* 2025; **15(3)**, 119-128.

[62] ETT Anton, GI Anton, IS Scripcariu, I Dumitrașcu, DV Scripcariu, IM Balmus, C Ionescu, M Visternicu and DG Socolov. Oxidative stress, inflammation, and antioxidant strategies in cervical cancer—a narrative review. *International Journal of Molecular Sciences* 2025; **26(10)**, 4961.

[63] T Kanaya, S Kyo and LA Laimins. The 5′ region of the human papillomavirus type 31 upstream regulatory region acts as an enhancer which augments viral early expression through the action of YY1. *Virology* 1997; **237(1)**, 159-169.

[64] W Wang, Z Yue, Z Tian, Y Xie, J Zhang, Y She, B Yang, Y Ye and Y Yang. Expression of Yin Yang 1 in cervical cancer and its correlation with E-cadherin expression and HPV16 E6. *PLoS One* 2018; **13(2)**, e0193340.

[65] E Grönroos, AA Terentiev, T Punga and J Ericsson. YY1 inhibits the activation of the p53 tumor suppressor in response to genotoxic stress. *Proceedings of the National Academy of Sciences* 2004; **101(33)**, 12165-12170.

[66] F Liang, S Kina, H Takemoto, A Matayoshi, T Phonaphonh, N Sunagawa, K Arakaki, A Arasaki, H Kuang and H Sunakawa. HPV16E6-dependent c-Fos expression contributes to AP-1 complex formation in SiHa cells. *Mediators of Inflammation* 2011; **2011**, 263216.

[67] SK Ghosh, T Sanyal and T Bera. Anticancer activity of solvent extracts of *Hexogonia glabra* against cervical cancer cell lines. *Asian Pacific Journal of Cancer Prevention* 2020; **21(7)**, 1977-1986.

[68] PY He, YH Hou, Y Yang and N Li. The anticancer effect of extract of medicinal mushroom *Sanghuangprous vaninii* against human cervical cancer cell via endoplasmic reticulum stress-mitochondrial apoptotic pathway. *Journal of Ethnopharmacology* 2021; **279**, 114345.

[69] AT Kiddane, MJ Kang, TC Ho, AT Getachew, MP Patil, BS Chun and GD Kim. Anticancer and apoptotic activity in cervical adenocarcinoma HeLa using crude extract of *Ganoderma*

applanatum. *Current Issues in Molecular Biology* 2022; **44(3)**, 1012-1026.

[70] C Loymunkong, K Panyawut, M Chaleesean and J Chuerduangphui. Potential water-based extracts from fresh and dried *Auricularia auricula-judae on* the inhibitory effect of human papillomavirus type 16 and cervical cancer cell line in CaSki. *Journal of Medical Pharmaceutical and Allied Sciences* 2022; **11(6)**, 5469-5475.

[71] CW Choi, JW Yoon, GH Yon, YS Kim, SY Ryu, SJ Seok, S Kang and YH Kim. Multidrug resistance reversal activity of methanol extracts from basidiomycete mushrooms in cancer cells. *Natural Product Sciences* 2012; **18(4)**, 239-243.

[72] MA Islam, MS Hossain, S Hasnat, MH Shuvo, S Akter, MA Maria, A Tahcin, MA Hossain and MN Hoque. *In-silico* study unveils potential phytocompounds in *Andrographis paniculata* against E6 protein of the high-risk HPV-16 subtype for cervical cancer therapy. *Scientific Reports* 2024; **14(1)**, 17182.

[73] P Strus, K Sadowski, W Ploch, A Jazdzewska, P Oknianska, O Raniszewska and I Mlynarczuk-Bialy. The effects of podophyllotoxin derivatives on noncancerous diseases: A systematic review. *International Journal of Molecular Sciences* 2025; **26(3)**, 958.

[74] SW Chiu, SC Law, ML Ching, KW Cheung and MJ Chen. Themes for mushroom exploitation in the 21st century: Sustainability, waste management, and conservation. *The Journal of General and Applied Microbiology* 2000; **46(6)**, 269-282.

Supplementary Material



Figure S1 Characteristics of *Russula emetica* fruiting body. *R. emetica* were collected from a tropical forest in Roi Et Province, Thailand. The basidiocarps exhibited reddish caps and white to slightly tinted cylindrical stipes.

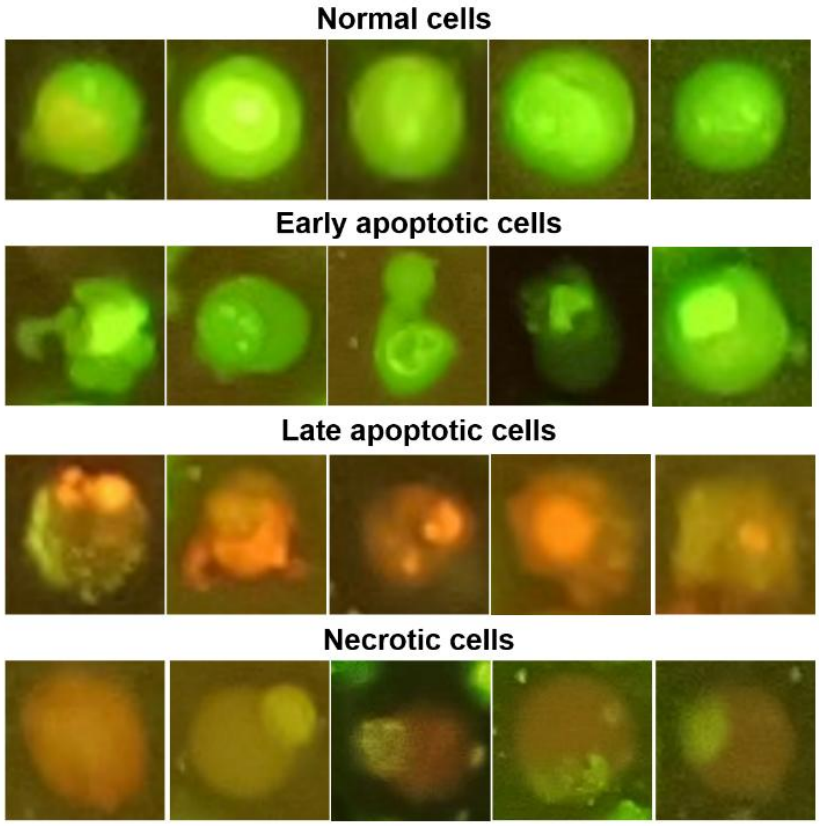


Figure S2 Criteria of cells exhibiting normal, early apoptotic, late apoptotic, and necrotic features in CaSki. The criteria to differentiate cell morphology of CaSki under acridine orange/ethidium bromide staining were as follows: cells with a normal nucleus with green fluorescence were considered normal; cells exhibiting plasma membrane blebbing with yellow or green fluorescence chromosomal condensation and concentration were classified as early apoptotic; cells with condensed chromatin showing orange to red fluorescence and cytoplasm ranging from green, to red were late apoptotic; and cells with increased cell volume and a uniformly orange-red nucleus were identified as necrotic.

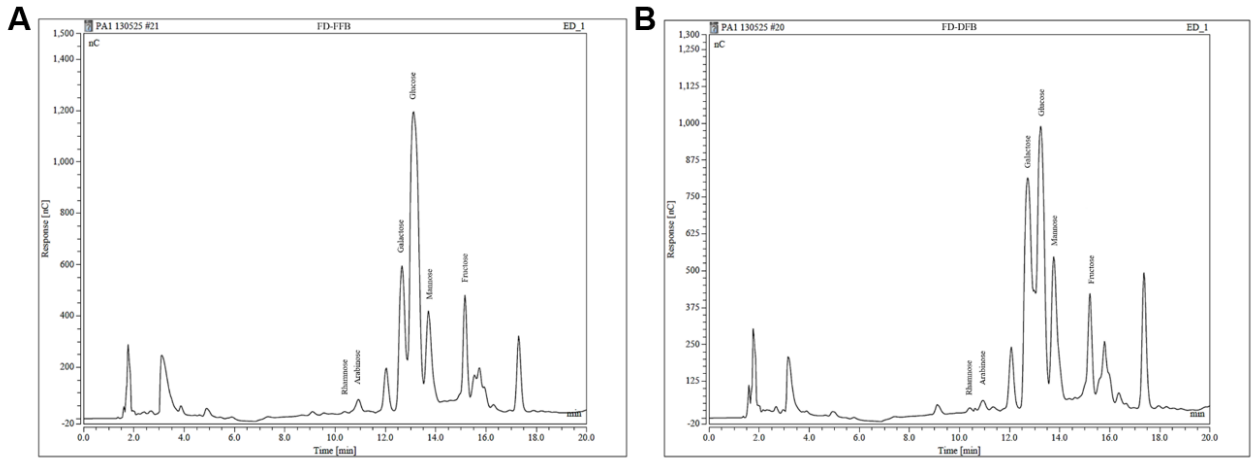


Figure S3 Chromatograms of arabinose, fructose, galactose, glucose, mannose, and rhamnose in FD-Fresh (A) and FD-Dried (B) analyzed by HPAEC.

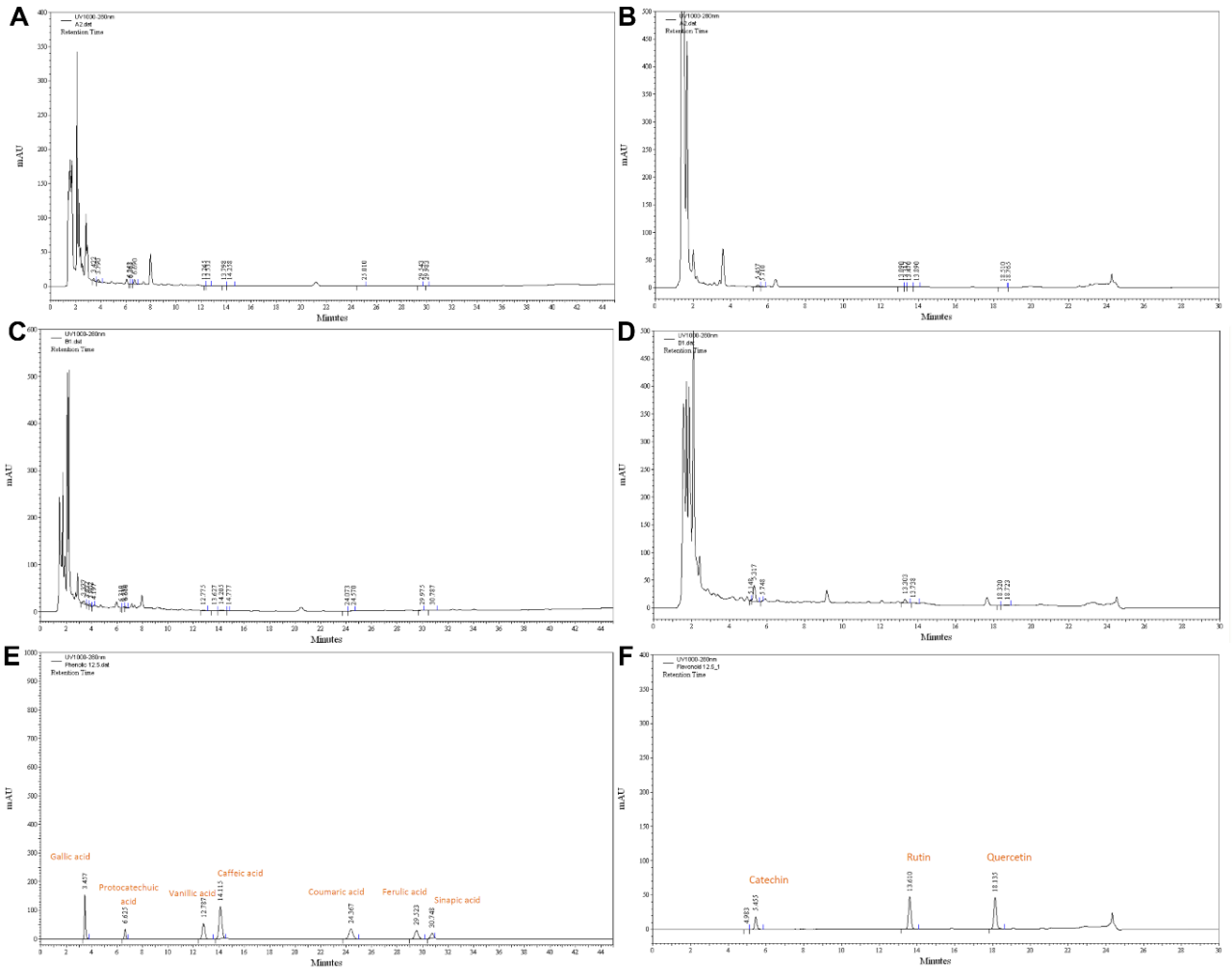


Figure S4 Chromatographic profiles of phenolic compounds and flavonoids of FD-Fresh and FD-Dried. Phenolic compounds of FD-Fresh (A), FD-Dried (B), and candidate standard profiles including caffeic acid, coumaric acid, ferulic acid, gallic acid, protocatechuic acid, sinapic acid, and vanillic acid (E). Flavonoid compounds of FD-Fresh (C), FD-Dried (D), and candidate standard profiles including catechin and quercetin (F).

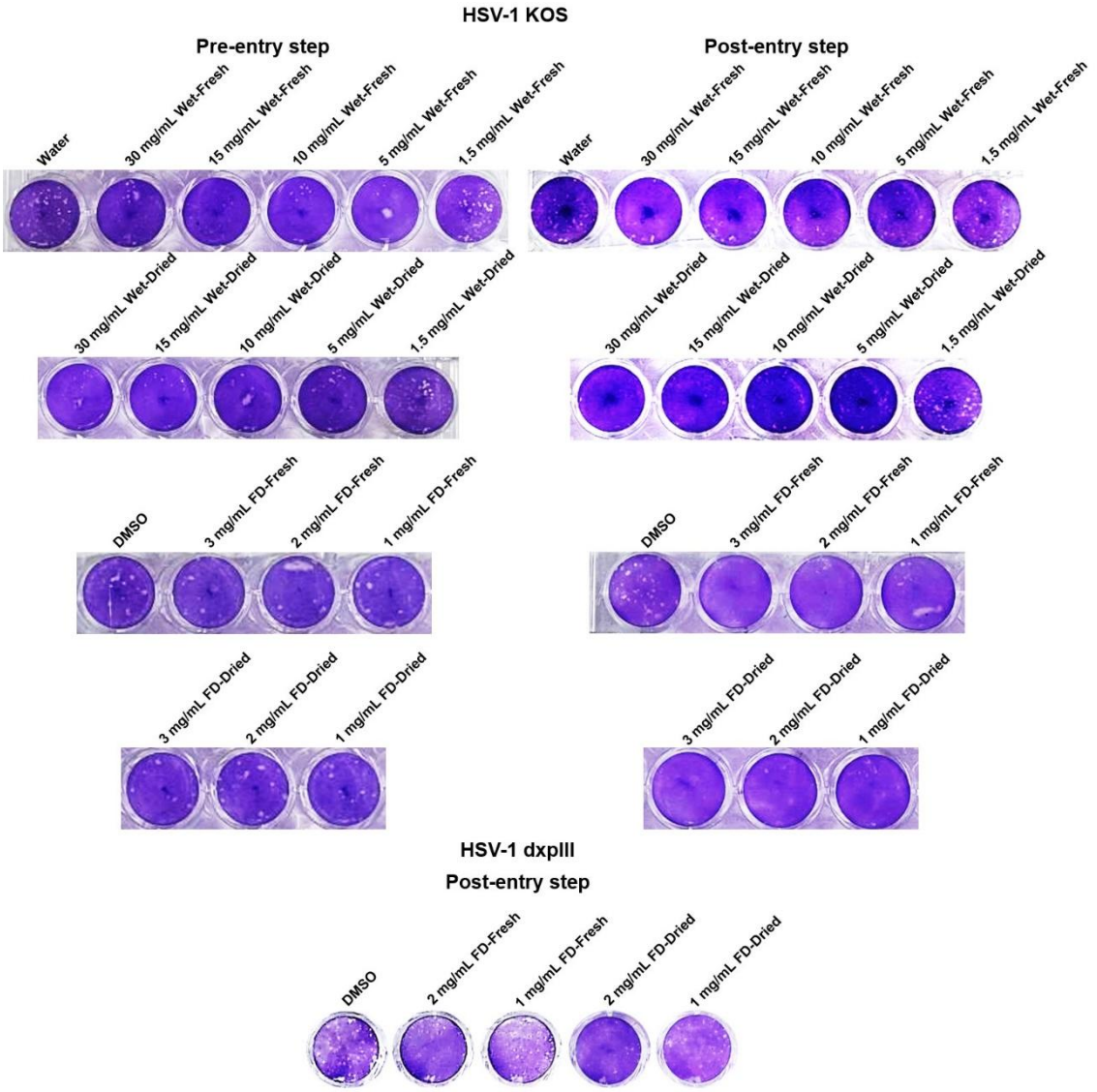


Figure S5 Plaque of *R. emetica* extract-treated cells in pre- and post-entry steps of HSV-1 KOS and dxpIII. The effects of *R. emetica* extracts were tested in Vero cells to investigate their antiviral activities against HSV-1 KOS at both pre- and post-entry steps, and against HSV-1 dxpIII at the post-entry step. Plaque formation was visualized by crystal violet staining at 48 and 72 h post-infection for HSV-1 KOS and HSV-1 dxpIII, respectively.

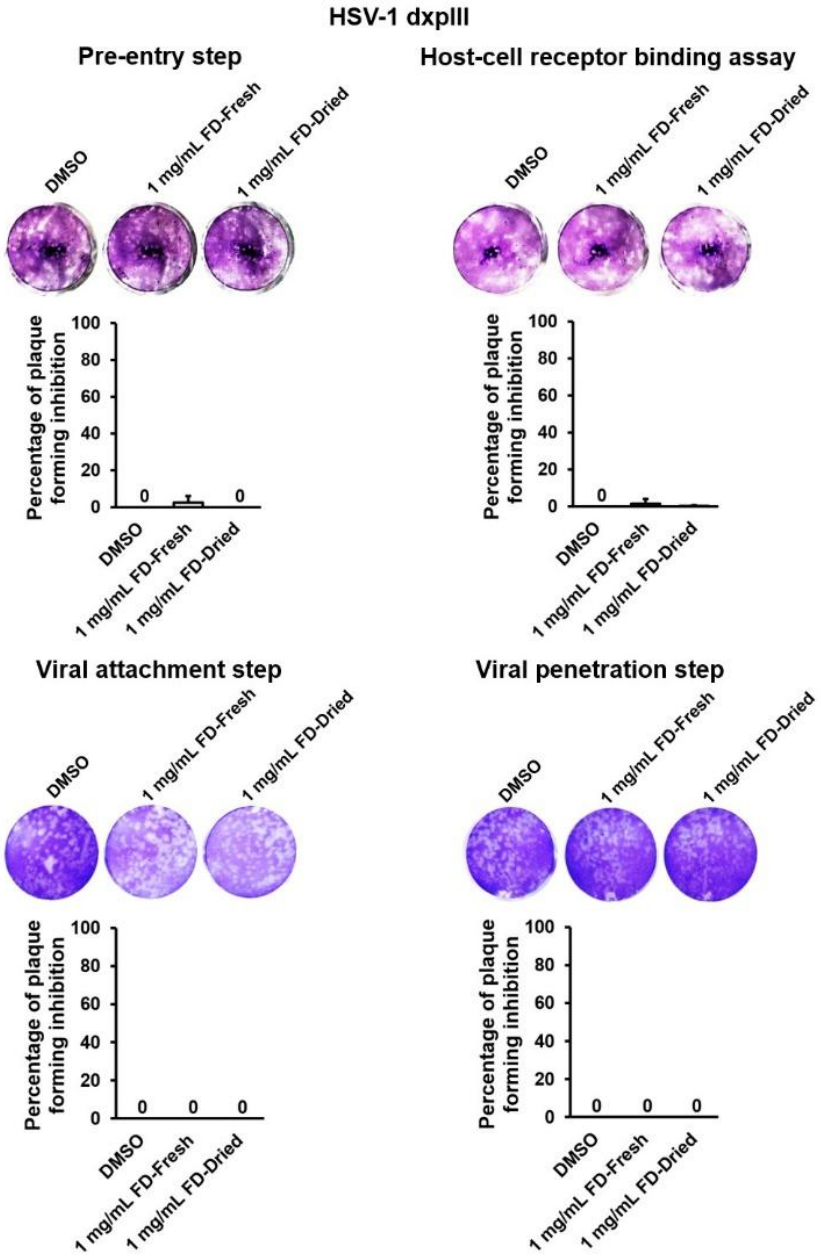


Figure S6 Plaque formation of HSV-1 dxpIII in *R. emetica* extract-treated cells across host-cell receptor binding, viral attachment, viral penetration, and pre-entry assays. The effects of *R. emetica* extracts were tested in Vero cells to investigate their antiviral activities against HSV-1 dxpIII at host-cell receptor binding, viral attachment, viral penetration, and pre-entry steps. For the host-cell receptor binding assay, the extracts were incubated with cells at 37 ºC for 1 h. Then, the extracts were removed, and the cells were infected with HSV-1 dxpIII (MOI 0.001) for 2 h at 37 ºC. The viruses were removed and replaced with the medium containing 0.4% carboxymethyl cellulose for 72 h. For the viral attachment assay, cells were pre-incubated at 4 ºC for 1 h. HSV-1 dxpIII (MOI 0.002) was mixed with the extract in a ratio of 1:1 and incubated at 4 ºC for 2 h. The viruses were removed and replaced with the medium containing 0.4% carboxymethyl cellulose for 72 h. For the viral penetration assay, cells were pre-incubated at 4 ºC for 1 h. HSV-1 dxpIII (MOI 0.001) was added to the cells and incubated at 4 ºC for 2 h. The viruses were removed and replaced with the extract, which was then continuously incubated at 4 ºC for 30 min, followed by immediate incubation at 37 ºC for 30 min. Then, cells were washed with PBS pH 3.0, 11.0, and 7.4, respectively, and continuously maintained in the medium containing 0.4% carboxymethyl cellulose for 72 h. The number of plaques in all assays were counted after crystal violet staining and used to calculate the percentage of viral inhibition. All experiments were performed independently in triplicate. The data are presented as mean ± SEM (n = 3 independent biological replicates, each measured in duplicate).

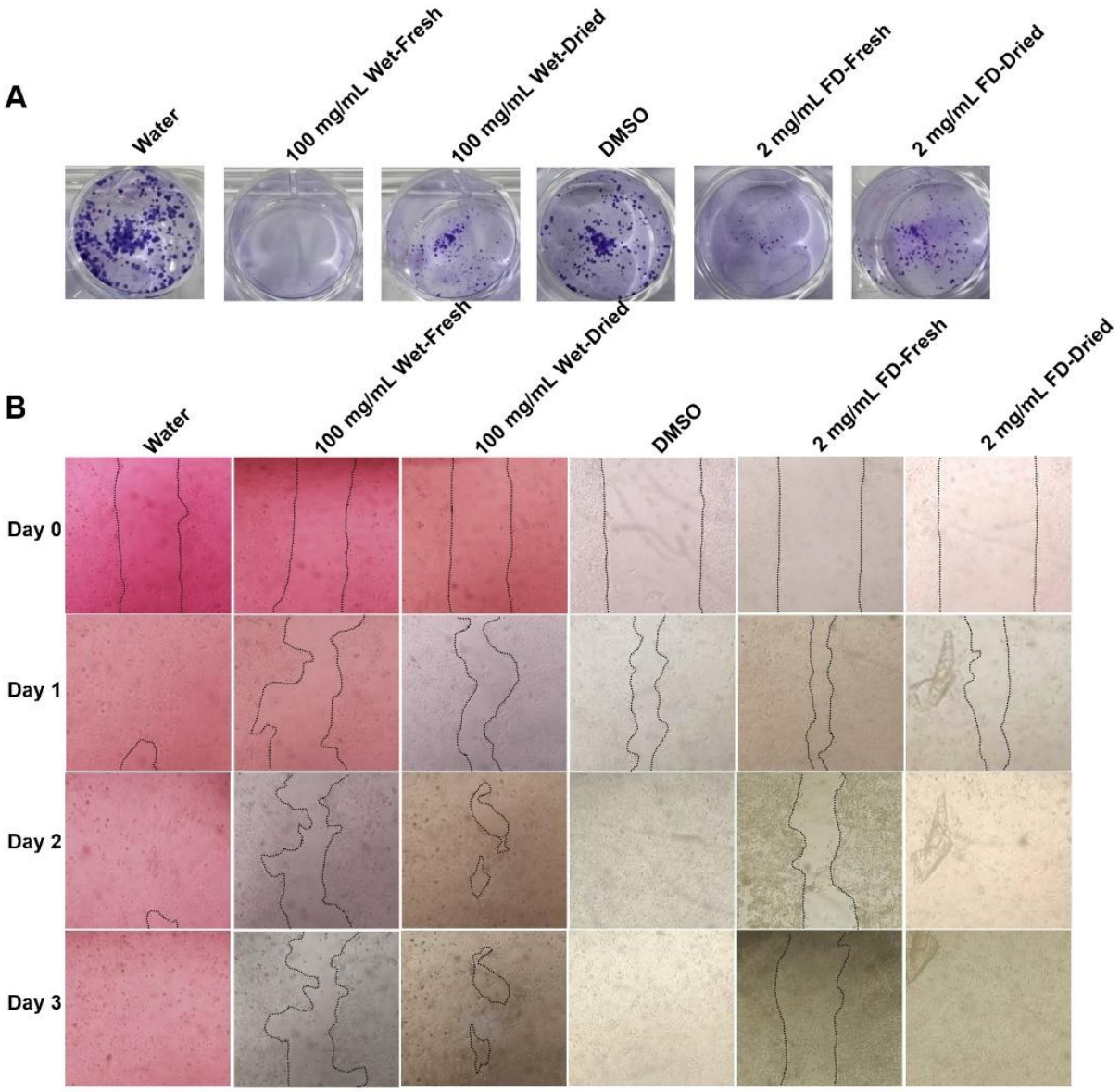


Figure S7 Colony forming and wound healing assays in CaSki treated with *R. emetica* extracts. Colony numbers and cell migration were performed in Wet-Fresh, Wet-Dried, FD-Fresh, and FD-Dried-treated CaSki using colony-forming (A) and wound healing (B) assays.

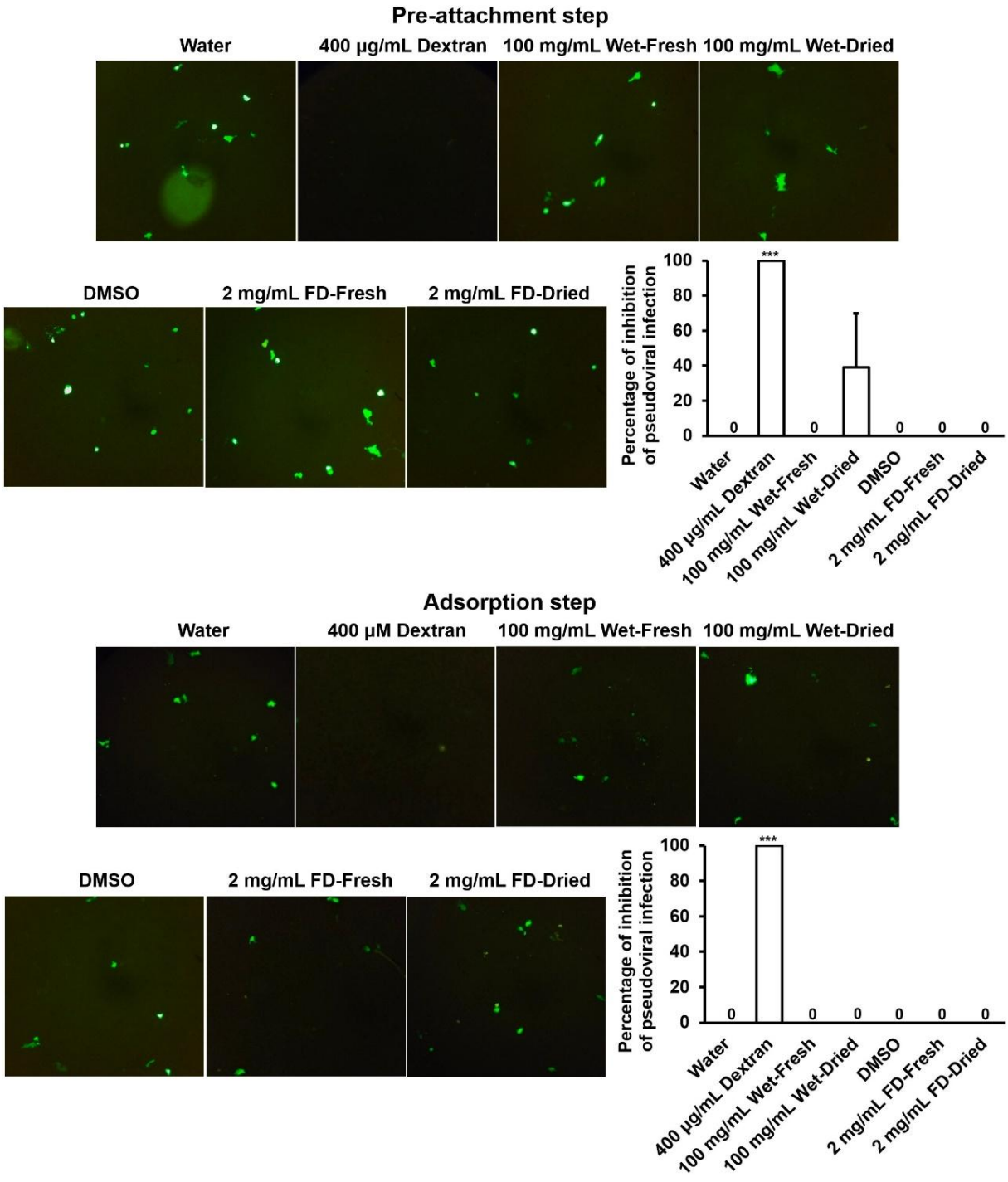


Figure S8 Effect of *R. emetica* extracts on anti-HPV-16 pseudovirus in pre-attachment and adsorption steps. HPV-16 pseudovirus was used to assay the pre-attachment and adsorption steps. Green fluorescent-expressing 293FT cells represent HPV16 pseudovirus infection. Total and green fluorescent-expressing cells were photographed under a light and fluorescent microscope. All data are presented as mean ± SEM (n = 3 technical replicates).

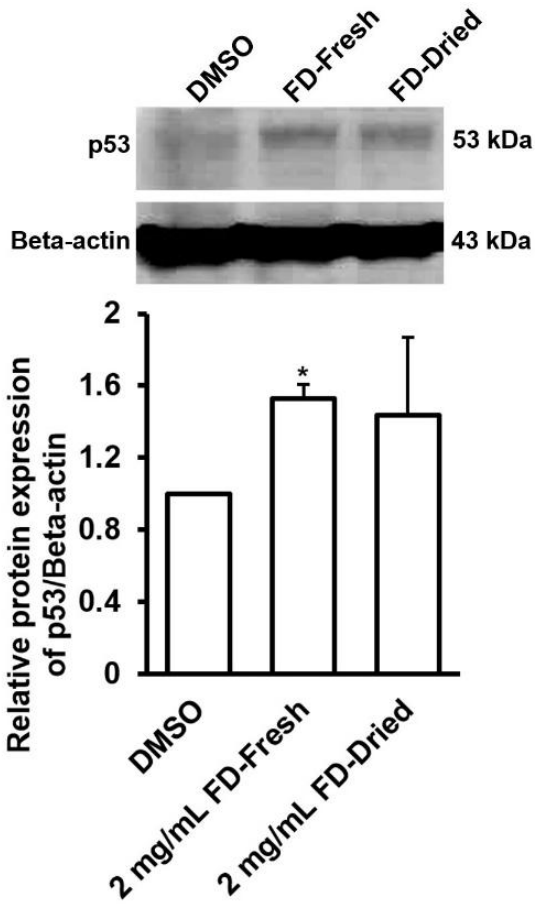


Figure S9 Effect of *R. emetica* extracts on p53 protein expression in CaSki. CaSki cells were treated with 2 mg/mL FD-Fresh and 2 mg/mL FD-Dried for 48 hours. The p53 and beta-actin proteins and intensities were detected using Western blot analysis and ImageJ software (version 1.54g), respectively. Data are presented as mean ± SEM (n = 3 independent biological replicates, each measured once.

Table S1 Primer sequences.

Primer	Sequence	Condition
c-FOS	Sense 5′-AGAATCCGAAGGGAAAGGAA-3′	45 cycles of 95 °C for 20 seconds and 60 °C for 30 seconds
	Antisense 5′-CTTCTCCTTCAGCAGGTTGG-3′	
GAPDH	Sense 5′-TCATCAGCAATGCCTCCTGCA-3′	
	Antisense 5′-TGGGTAGCAGTGATGGCA-3′	
HPV-16E6	Sense 5′-TCAAAAGCCACTGTGTCCTG-3′	
	Antisense 5′-CAGCTGGGTTTCTCTACGTGT-3′	
HSV gD	Sense 5′-CTATGACAGCTTCAGCGCCGTCAG-3′	
	Antisense 5′-CGTCCAGTCGTTTATCTTCACGAGC-3′	
UL30	Sense 5′-GTGTTGTGCCGCGGTCTCAC-3′	
	Antisense 5′-GGTGAACGTCTTTTCGAACTC-3′	
YY1	Sense 5′-TTGCTCAGTCAACTAACCTGAAATC-3′	
	Antisense 5′-GAGGCATATTTATTCCCAATCACAC-3′	

Table S2 Cytotoxic concentrations at 50% (CC_{50}) of *R. emetica* extracts in 293FT, Vero, CaSki and SiHa cell lines.

Cell line	CC_{50} (mg/ml)			
	Wet-Fresh	**Wet-Dried**	**FD-Fresh**	**FD-Dried**
293FT	> 250	> 250	> 10	> 10
Vero	171.73 ± 0.13[a]	200.16 ± 0.12[b]	10.91 ± 0.55[c]	> 10
CaSki	106.06±0.22[a]	146.22±0.03[b]	4.44±0.27[c]	9.43±1.15[d]
SiHa	130.56±0.03[a]	170.96±0.01[b]	6.45±0.87[c]	14.27±0.91[d]

Note: Different lowercase letters (a–d) indicate significant differences among these 4 extracts. All data are presented as mean ± SEM ($n \geq 3$ independent biological replicates, each measured in triplicate).